View Article Online
View Journal

Energy & Environmental Science

Accepted Manuscript

This article can be cited before page numbers have been issued, to do this please use: J. Zhao, X. Fan, H. Xie, Y. Luo, Z. Li, X. Peng, G. Tao, Z. L. Wang and K. Dong, *Energy Environ. Sci.*, 2025, DOI: 10.1039/D5EE00144G.

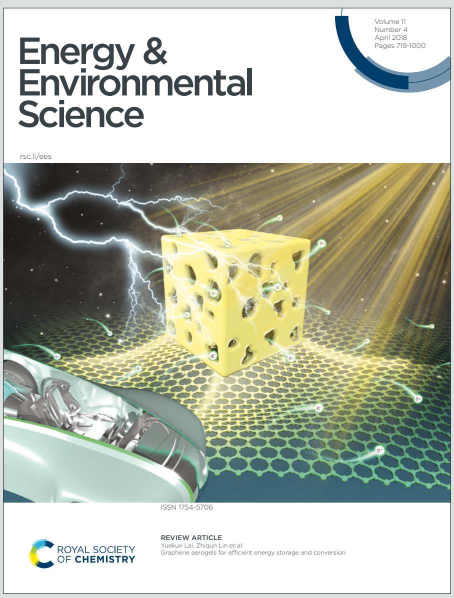

ROYAL SOCIETY OF CHEMISTRY

rsc.li/ees

View Article Online
DOI: 10.1039/D5EE00144G

Broader context statement:

In contemporary society, numerous electronic products have become essential daily wearables. However, the supply of energy and the acquisition of sensing information have emerged as critical challenges. Traditional bulky batteries struggle to meet the power requirements of wearable devices anytime and anywhere. Utilizing everyday clothing accessories to convert bodily movement into electrical energy and sensing information in real-time presents a promising solution to these demands. This approach requires highly efficient harvesting of low-frequency, irregular mechanical energy generated by body movements and ensuring comfort, breathability, safety, and durability. Mechano-electric conversion fibers (MECFs) have been developed based on triboelectric nanogenerator technology and utilizing novel smart textile materials. MECFs can transform mechanical energy produced by human activities into electrical energy, achieving self-sufficient power supply and self-powered sensing. MECFs give rise to a self-sustaining energy ecosystem centered around the human body. Within this system, humans act both as the "producers" and "consumers" of energy and information. This groundbreaking system not only enhances the practicality of wearable devices but also injects momentum into fields such as artificial intelligence, the Internet of Things, and human-machine interfaces, significantly propelling the advancement towards smarter lifestyles.

View Article Online
DOI: 10.1039/D5EE00144G

Revolutionizing Wearable Sustainable Energy Enabled by Mechano-Electric Conversion Fibers

Jizhong Zhao[1,2], Xiaoxuan Fan[1,2], Hongxiang Xie[1,3], Yi Luo[1,4], Zhifeng Li[1,2], Xiao Peng[5], Guangming Tao[6,], Zhong Lin Wang[1,7,*], Kai Dong[1,2,*]*

[1]`Beijing Institute of Nanoenergy and Nanosystems, Chinese Academy of Sciences, Beijing 101400, PR China
[2] School of Nanoscience and Technology, University of Chinese Academy of Sciences, Beijing 100049, PR China
[3] College of Textile and Clothing, Xinjiang University, Urumqi 830046, P R China
[4] School of Integrated Circuits, Dalian University of Technology, Dalian 116024, P R China
[5] Key Laboratory of Organic Optoelectronics and Molecular Engineering of the Ministry of Education, Department of Chemistry, Tsinghua University, Beijing 100084, PR China
[6] Wuhan National Laboratory for Optoelectronics and School of Optical and Electronic Information, Huazhong University of Science and Technology, Wuhan, 430074, PR China
[7] Georgia Institute of Technology, Atlanta, Georgia 30332-0245, USA
*Email: tao@hust.edu.cn, zhong.wang@mse.gatech.edu, dongkai@binn.cas.cn

Abstract

Mechano-electric conversion fibers (MECFs) represent a groundbreaking innovation in smart textiles, integrating the high-efficiency mechanical energy conversion of triboelectric nanogenerators (TENGs) with superior wearability and comfort inherent in textile materials. Despite notable advancements in MECFs, comprehensive reviews and in-depth discussions of their fundamental principles and unique advantages remain scarce. Herein, this review aims to bridge this gap by providing a systematic analysis and objective outlook of MECFs, with a particular emphasis on their transformative potential in revolutionizing energy harvesting and self-powered sensing in human-centered applications. Driven by diverse structural designs, abundant material selection configurations, and high conversion efficiency at low frequencies, MECFs have developed a self-sufficient human surface energy supply-demand system that is autonomous, sustainable and undisturbed. Their high sensitivity is underpinned by a multilinear dynamic progressive response mechanism, facilitating rapid response times and high sensitivity across a wide spectrum of mechanical stimuli. In addition, the prominent applications of MECFs in self-powered wearable sensing are also explored, including personalized healthcare monitoring, human-machine interacting, and smart security protecting. Finally, we discuss in detail the key challenges and bottlenecks that still exist in MECF development, alongside promising solutions and future development directions. This work seeks to establish a comprehensive knowledge theoretical framework for MECFs and accelerate their transition from fundamental research to large-scale practical

View Article Online
DOI: 10.1039/D5EE00144G

applications.

Keywords
mechano-electric conversion fibers and textiles, triboelectric nanogenerators, wearable electronics, self-powered sensing, personalized healthcare monitoring

1. Introduction

In recent years, mobile smart devices, health monitoring systems and other customized services have significantly penetrated our daily lives, and the number of wearable electronics required for daily human needs is rapidly increasing, leading to an increasingly important demand for sustainable human body energy.[1,2] However, traditional portable rigid battery components are unable to achieve sustained and stable power supply in scenarios with inconvenient power supply, due to their large and bulky volume, limited storage capacity, and frequent charging requirements.[3-5] Mechanical energy, as a widely distributed and diverse form of human body energy, is often overlooked or discarded due to its irregularity, dispersion, and low energy density characteristics. High efficiency collecting the disordered human body energy and then converting it into electricity is considered a promising solution to meet the continuous and stable power supply of wearable electronics. Developing smart wearable devices with multiple functions such as health monitoring, intelligent interaction, personal protection, and most importantly, no need for an external power supply, is an ideal approach to meet the demands of artificial intelligence (AI), Internet of Things (IoTs),[6-9] and human-machine interfaces (HMI) for individual consumers.[10,11] Mechano-electric conversion fibers (MECFs) are a new type of smart textiles developed according to the above concept, with the outstanding functions of autonomous power supplying and self-powered sensing. The efficiency of MECFs in harvesting low-frequency and irregular mechanical energy from the human body is significantly higher than that of traditional electromagnetic generators (EMGs), which may help eliminate reliance on batteries and other power supply devices.[12] Therefore, MECF is closely linked to the wearer, who acts as both the "producer" of electrical energy and the "consumer" of electrical energy demand (**Figure 1**). Under this paradigm, the human body functions not only as an inexhaustible source of electrical energy but also as the ultimate application platform for wearable electronics. As a result, MECF can establish a self-sustaining energy supply-and-demand system tailored to the human body.

View Article Online
DOI: 10.1039/D5EE00144G

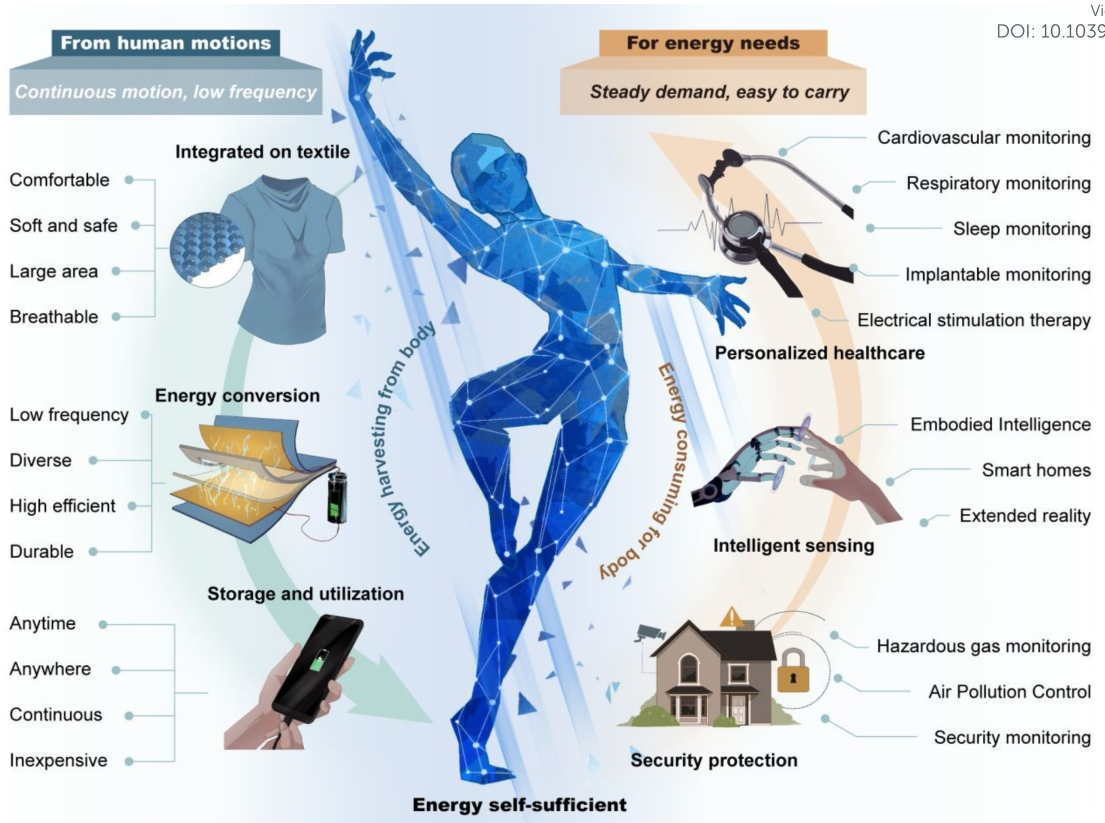

Figure 1. The development concept of MECFs. MECFs, owing to their fabric properties, are highly suitable for being worn. Their working principle allows for efficient energy harvesting, and the energy thus harvested can effectively meet the power consumption requirements of electronic products. MECFs find extensive application scenarios in three major fields: personalized healthcare, intelligent sensing, and safety protection. This innovative self-sufficient approach enables efficient mechanical energy collection and power wearable electronics. This concept bridges the gap between energy generation and utilization, propelling the development of sustainable, body-integrated technologies.

2. Mechanism of MECF

2.1 Quantitative Model of TENG's Output

MECF is an ideal option for harvesting human body energy to power wearable electronic devices, leveraging the operational principles of the triboelectric nanogenerator (TENG). A TENG typically consists of two material layers or fibers with distinct triboelectric properties: one exhibits positive triboelectricity (electron donor), while the other exhibits negative triboelectricity (electron acceptor). Through contact electrification (CE), charges are generated on these two materials, and then they contact and separate under the drive of mechanical motion. Charge transfer occurs between the two materials under periodic contact and separation driven by mechanical forces, leading to charge accumulation (**Figure 2**a). In systems with defined boundaries and volumes, such as conventional electromagnetic devices, their behaviors can be described by the standard Maxwell's equations.[13] However, due to the dynamic materials and transient configurations to TENGs, the classical Maxwell's

DOI: 10.1039/D5EE00144G

equations require extension to accommodate these unique characteristics. Building upon the integral formulation of Maxwell's equations under the assumptions that the volume of the medium and its surface or interface are fixed and the medium undergoes translational motion as a rigid body, Prof. Wang derived a standard differential form of expanded Maxwell's equations (1a–1d) specifically tailored to TENGs:[14]

$$\nabla \cdot \boldsymbol{D} = \rho \tag{1a}$$

$$\nabla \cdot \boldsymbol{B} = 0 \tag{1b}$$

$$\nabla \times \left(\boldsymbol{E} + \boldsymbol{v}_{\mathrm{r}} \times \boldsymbol{B}\right) = -\frac{\partial}{\partial t}\boldsymbol{B} \tag{1c}$$

$$\nabla \times \left(\boldsymbol{H} - \boldsymbol{v}_{\mathrm{r}} \times \boldsymbol{D}\right) = \boldsymbol{J} + \rho \boldsymbol{v} + \frac{\partial}{\partial t}\boldsymbol{D} \tag{1d}$$

where $\rho\boldsymbol{v}$ represents the current density generated due to the translational motion of the medium (Figure 2b). The extended Maxwell's equations provide a more accurate framework for analyzing and predicting the performance of TENG in practical applications. Owing to CE effect, the medium accumulates a certain amount of static charge in advance. Consequently, when the shape of the medium or the moving object changes, it not only leads to variations in local charge density over time but also generates a local "virtue" current density. To accurately describe these two charge effects, it is necessary to modify the displacement vector $\boldsymbol{D}$ by adding an additional term $\boldsymbol{P}_{\mathbf{s}}$ to represent the polarization phenomenon caused by the pre-existing static charges on the medium.[15] Therefore, the expression of the modified displacement vector is:

$$\boldsymbol{D} = \varepsilon_0 \boldsymbol{E} + \boldsymbol{P} + \boldsymbol{P}_{\mathrm{s}} = \varepsilon_0 (1+\chi)\boldsymbol{E} + \boldsymbol{P}_{\mathrm{s}} \tag{2}$$

where ε_0 is the vacuum permittivity and $\boldsymbol{E}$ is the electric field strength. In this model, $\varepsilon_0\boldsymbol{E}$ corresponds to the electric field generated by free charges, usually called the external electric field and polarization vector $\boldsymbol{P}$ describes the polarization phenomenon inside the medium caused by the external electric field $\boldsymbol{E}$. The added term $\boldsymbol{P}_{\mathrm{s}}$ mainly reflects the existence of surface static charges and the change of boundary shape over time. $\boldsymbol{P}_{\mathrm{s}}$ is neither free nor polarization charges caused by the electric field but refers to the inherent bound electrostatic charges introduced on the surface of the medium triggered by external mechanical actions, making them unique components of the TENG system. This term is crucial for advancing the theory of mechanical-to-electrical energy conversion because it accurately describes how mechanical motion generates and transmits charges, thereby achieving efficient conversion from mechanical to electrical energy.[16] The extended equations explicitly describe how mechanical motions (e.g., fiber deformation, sliding) alter the local charge density and induce displacement currents. This enables researchers to predict output performance under different mechanical stimuli (e.g., frequency, amplitude) and optimize the fiber arrangement for specific applications (e.g., vertical contact - separation mode vs. lateral sliding mode). Such modifications enhance the applicability of Maxwell's equations to TENG systems with moving materials and

View Article Online
DOI: 10.1039/D5EE00144G

transient configurations, thus more accurately reflecting their working principles and dynamic behavior and further advances the development of the entire TENG field (Figure 2c).

2.2 Microscopic Mechanism of Energy Conversion

The CE is commonly observed between materials with markedly different physical and chemical properties (Figure 2d), and the greater the disparity in their electron affinity, the more pronounced the effect tends to be. As the theory of CE has evolved, two models have been proposed to explain this phenomenon: the surface state model and the electron-cloud-potential-well model.[17] The surface state model aids in elucidating the mechanism of CE, particularly in materials characterized by band structures (Figure 2e).[18] The presence of a solid surface disrupts the periodicity of the crystal lattice, leading to the creation of new energy states within the bandgap. Surface defects can influence the occupation of these states by electrons. As shown in Figure 2a, different materials, due to their distinct valence band positions, occupy different surface state energies. When two materials come into contact, the energy differences between these surface states drive electron transfer, resulting in CE. The surface state model emphasizes that the static charges generated during CE are bound to the surface states and may not be free to move, especially in materials with low electrical conductivity. These charges are expected to remain on the surface permanently, but thermal fluctuations can release trapped electrons, as described by the thermionic emission model.[19] The occupation and transfer of electrons play a crucial role in the generation of static charges during CE. Typically, the surface state model is applicable to dielectric materials with surface defects, which can be explained using band diagrams. However, for materials whose electronic structure is represented by molecular orbitals, especially for polymers, the surface state model becomes inadequate. In such cases, the electron-cloud-potential-well model is used to explain CE phenomena.

The electron-cloud-potential-well model suggests that when two materials come into contact, their respective electron clouds overlap due to the applied external force (Figure 2f). This overlap leads to the formation of ionic or covalent bonds between the materials, causing electron transfer and resulting in CE.[20] A and B represent atoms from two different materials and the nucleus surrounded by negatively charged electron clouds. The spatial distribution of electrons is intrinsically linked to the potential wells associated with the atoms. When the two materials approach each other, their electron clouds overlap and begin to interact, which modifies the original single potential wells into an asymmetric double-well structure, and reduces the barrier.[4] This transformation establishes an energy gradient that enables electrons to migrate from higher-energy states to lower-energy states, thereby causing CE. These theoretical insights not only provide a scientific basis for the design of TENGs but also lay the foundation for further optimizing their performance.

View Article Online
DOI: 10.1039/D5EE00144G

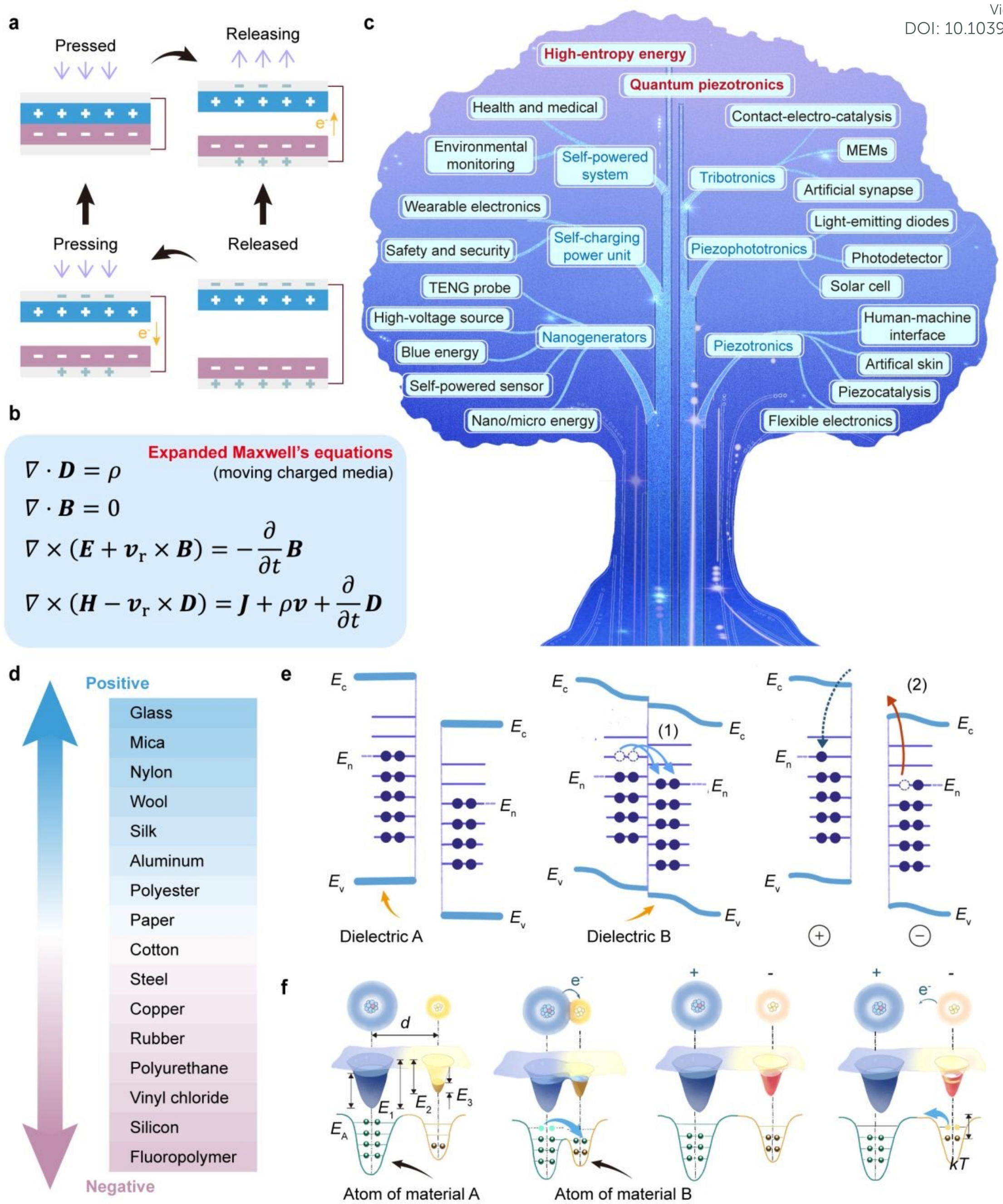

Figure 2. The computational models and microscopic mechanisms of TENGs. a) During operation, the two charged dielectric materials in a TENG undergo mechanical motion. b) Expanded Maxwell's equations for moving charged media. c) Application areas of TENG in various fields. d) Triboelectric series of materials. e) The surface state model. f) The electron-cloud-potential-well model.

2.3 Optimization of TENG Performance

Enhancing the performance of TENGs is crucial for expanding their applications and accelerating industrial adoption. Optimization strategies focus on two main areas: increasing the material's inherent charge output capability (material modification and charge injection techniques) and reducing charge dissipation during operation. First, material modification includes both physical and chemical approaches. Physical

View Article Online
DOI: 10.1039/D5EE00144G

modification involves triboelectric material's microstructure construction and dielectric charge doping.[21] Chemical methods, such as surface functionalization and grafting functional groups, further improve the triboelectric effect. The chemical structure and density of functional groups influence the highest occupied molecular orbital (HOMO) energy levels, a key factor in regulating the charging behavior of negative and positive triboelectric polymers.[22] For instance, halogen and amine monomers, with their strong electron-withdrawing and donating abilities, are commonly used due to their high polarity. Fluorine, chlorine, imides, and siloxanes can enhance negative triboelectric properties, while amides, ureas, nitrile groups, and amino resins are suitable for positive triboelectric polymers. Charge injection techniques, including corona polarization, irradiation, and charge self-injection, introduce electrons or ions into the dielectric film surface to compensate for limited triboelectric charging. [23] However, injected charges primarily reside in the shallow surface layers, making them susceptible to significant loss from air breakdown and rapid decay due to trap states.

Second, managing charge dissipation is equally important. Charge dissipation occurs through three main pathways: atmospheric ion neutralization, surface conduction, and bulk conduction. Atmospheric ion neutralization happens when charged ions or water molecules gather on the polymer surface, forming conductive paths that lead to charge leakage and reducing effective charge storage.[24] Surface conduction arises from the diffusion of surface charges driven by concentration gradients of injected charges, along with downward migration due to charge leakage within the dielectric polymer, ultimately causing a decline in TENG output. Bulk conduction within the polymer depends on the trap states, where the energy levels and density of these traps determine the polymer's ability to capture and retain charges. In TENGs, charges are stored and released through shallow traps and deep traps.[28-30]The ratio of deep to shallow traps significantly affects the rate of charge dissipation and deep traps are more effective at capturing and retaining charges, while shallow traps contribute to faster charge loss. Several strategies have been proposed to mitigate charge dissipation. Optimizing trap distribution by incorporating high-charge-capturing materials like TiO_2 increases the concentration of deep traps.[25] Constructing charge transfer channels using highly conductive materials, such as PVA, stores surface charges deeper within the dielectric layer.[26] Building charge blocking layers with low-leakage and strong charge-capturing materials, high-dielectric ceramics for example, prevents the neutralization of drifting charges with induced charges at the bottom electrode.[27] At the same time, the humidity and temperature in the operating environment can also be controlled to reduce air breakdown and charge drift. Adjusting the operating voltage to avoid excessive voltage that could lead to air breakdown is also effective. Addressing charge dissipation and optimizing material properties, researchers can significantly improve TENG performance and broaden its application and innovation scope.

3. Output Characteristics of MECF

3.1 Hierarchical Structure of The Textiles

View Article Online
DOI: 10.1039/D5EE00144G

MECF can effectively convert small and irregular mechanical energy into electrical power, with variations in the generated electrical signals closely correlated to mechanical stimuli. This enables MECFs to achieve the collection, conversion, and utilization of various forms of mechanical energy.[28] Based on the circuit connection methods and the direction of the applied load, the design of MECFs encompasses four fundamental working modes of TENGs, including vertical contact-separation mode, lateral sliding mode, single-electrode mode, and freestanding triboelectric-layer mode.[29] Vertical contact-separation mode is the most common design for MECFs and offers strong versatility (**Figure 3**a-i). It can be applied to both planar surfaces and fibers, making it particularly suitable for capturing signals that occur perpendicular to the working plane.[30] Monitoring various pressure signals, for instance, the interaction between foot and the ground during running or jumping is ideal for this mode. Similar in structure to the vertical contact-separation mode, the lateral sliding mode differs in that the motion direction changes from vertical to in-plane sliding (Figure 3a-ii). This design is well-suited for monitoring physical quantities such as displacement, angular changes, and acceleration.[31] For example, it can effectively capture the friction between a swinging arm and the body while running. In the single-electrode mode, one of the films and its corresponding electrode are removed, leaving the remaining electrode connected to ground (reference potential). This design is structurally simpler with higher flexibility and ability to overcome spatial constraints (Figure 3a-iii),[32] though it may generate half the charge compared to other modes. The freestanding triboelectric-layer mode does not require grounding, as all electrodes are free to move. This design closely resembles the lateral sliding mode in terms of application range (Figure 3a-iv).[33] By leveraging these different working modes, TENG can be tailored to specific applications.[34] Integration with fabric allows textile-based TENGs to have excellent mechanical flexibility, breathability, moisture permeability, and design potential to meet the demands of personalized wearable electronics (Figure 3b).[35-37] From the perspective of fiber orientation and structural dimensions, textiles are primarily categorized into fibrils assemblies,[38] 1D yarns, 2D textiles, and more complex 3D structures.[39] Fibrils are the fundamental components of the textile. By employing various techniques along their axial direction, thousands of fibers can be assembled/interlocked to form 1D yarns. 1D yarns can be further integrated into 2D or 3D fabrics by means of weaving,[40,41] knitting,[42,43] stitching, braiding, and winding,[44,45] etc. 2D woven structures are the most widely used in the textile industry which can be further divided into plain, twill, and satin while 2D knitted structures include weft knitting and warp knitting. Besides, braiding and nonwoven are also common manufacturing processes. Braiding is the simplest type of woven structure, achieved by intertwining two yarns in an offset direction.[46] Nonwoven fabrics are a fabric-like material made from discontinuous short fibers or filaments that are entangled in a random orientation.[47] If another longitudinally oriented yarn system is inserted into the biaxial structure, a 3D structure is obtained.[48,49] The multi-layered fiber distribution can create more contact-separation spaces, effectively improving the power output density of textile TENGs.[50] These vast design spaces make textiles an excellent carrier for integrating smart electronic devices. This combination means that

View Article Online
DOI: 10.1039/D5EE00144G

the energy generated from human movements, such as walking, jumping, or muscle contractions (Figure 3c), can be harvested and converted into electrical energy by MECFs (Figure 3d). The collected energy will power devices, such as LEDs, smartwatches, thermometers, calculators, etc.[51-53]

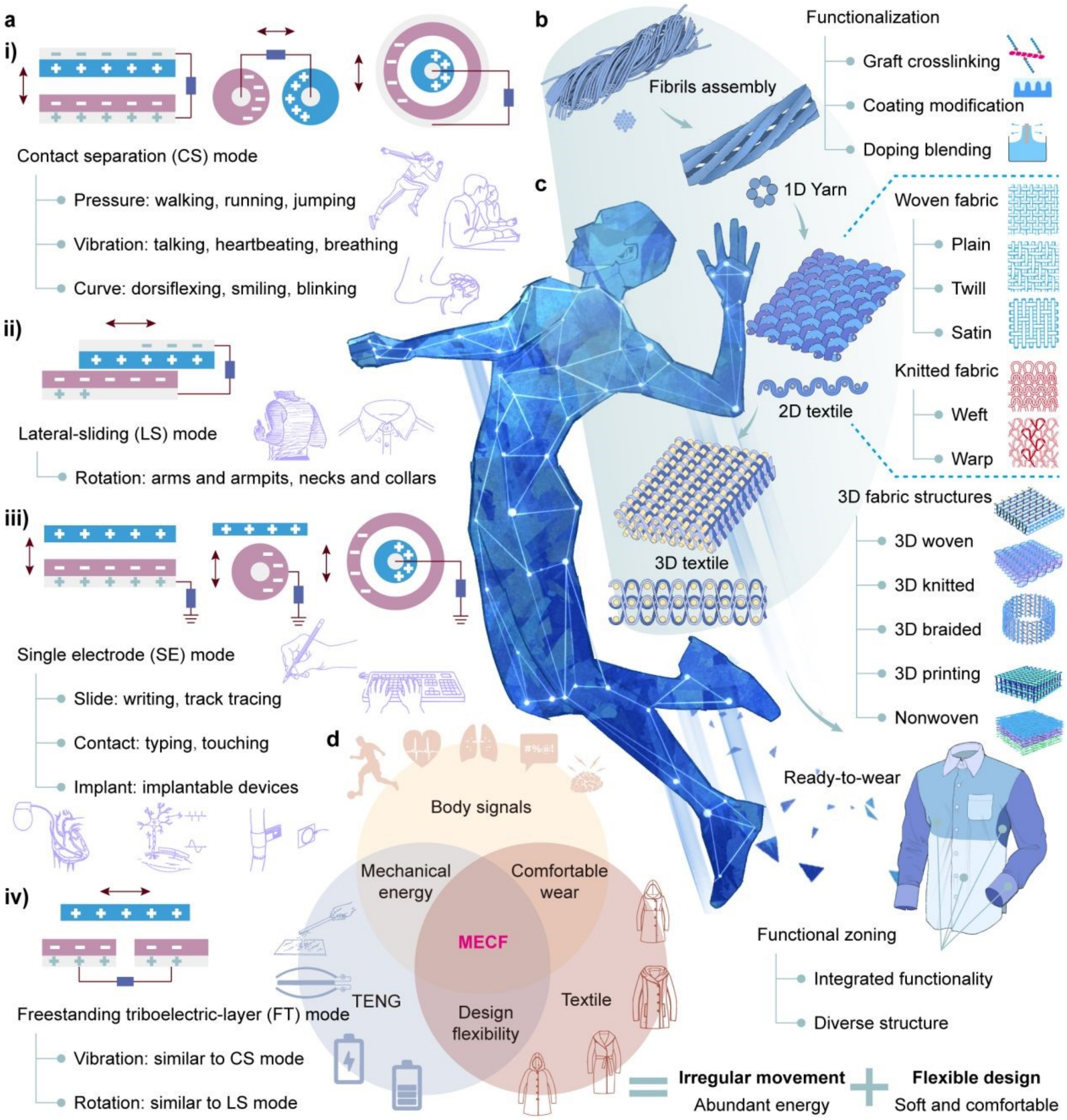

Figure 3. The structural design and key features of MECFs. a) Four fundamental working modes of TENGs, including i) vertical contact-separation mode, ii) lateral sliding mode, iii) single-electrode mode, and iv) freestanding triboelectric-layer mode. b) Diversified structural design potential of fibers, yarns, and textiles. c) Human motion. d) MECF is an ideal solution that utilizes TENGs combined with textiles to harvest human body energy and meet the energy needs of wearable electronics.

3.2 Materials and Fabrication Processes

Triboelectric materials play a critical role in determining the performance of MECFs. The triboelectric output increases with the separation distance between two materials in the triboelectric series.[54] Various methods have been developed to

View Article Online
DOI: 10.1039/D5EE00144G

fabricate and modify triboelectric materials, including ion etching, block copolymer techniques, templating, self-assembled monolayers, and ion implantation. Recent research has focused on natural material as tribo-positive layer in MECFs. Cellulose, the most abundant natural material worldwide, is widely studied due to its abundance, low cost, renewability, and biodegradability.[11] Chitosan, structurally similar to cellulose, replaces the hydroxyl group (-OH) at the C-2 position with an amino group (-NH_2). The electron-donating tendencies of -OH and -NH_2 functional groups make chitosan more tribo-positive than cellulose.[55,56] Cotton fabrics can also serve as effective tribo-positive materials.[57] Beyond biomass materials, synthetic fibers such as thermoplastic polyurethane (TPU) fibers, known for their broad tensile strain range, excellent mechanical properties,[58] can be modified with additives like mica flakes,[59] to improve triboelectric output. Natural rubber, a widely used tribo-negative material, is characterized by high elasticity, low thermal conductivity, electrical insulation, and biodegradability.[60] Polyvinylidene fluoride (PVDF) and its modified fibers, including graphene nanoparticle (GNP)-doped PVDF,[61] perovskite barium zirconium titanate (BZT)-filled polyvinylidene fluoride-co-hexafluoropropylene (PVDF-HFP),[62] and in situ-deposited styrene ethylene butylene styrene (SEBS) microsphere-modified PVDF-HFP,[63] exhibit significantly enhanced outputs compared to pure PVDF. Polyacrylonitrile (PAN) fibers, another common tribo-negative materials,[64] are extensively used in carpets, sportswear, sails, and military fabrics. The contact between electrodes and triboelectric materials in MECFs is crucial for ensuring the accuracy and stability of output signals. MXenes, a family of two-dimensional (2D) transition metal carbides, carbonitrides, or nitrides, have attracted attention for their metallic conductivity, abundant active sites, and potential applications in batteries, capacitors, and MECFs.[65] Carbon-based materials such as carbon nanotubes (CNTs), carbon nanoparticles, carbon fibers, and graphene are also widely employed as electrodes in MECFs due to their simple fabrication processes and low cost.[66,67] Traditional electrodes like silver and copper face challenges in flexibility and wash durability. In contrast, conductive polymer fibers, such as 3,4-ethylenedioxythiophene:polystyrene sulfonate,[68] offer high conductivity, strong adhesion, and resistance to bending and machine washing.

Textile manufacturing techniques are frequently adapted for MECF production. Conventional spinning processes, for example, are used to twist fibers around core yarns, forming multi-strand composite structures.[69,70] Electrospun MECFs are typically categorized into nonwoven fabrics,[71] or coaxial electrospun yarns,[40] with microstructured designs further improving device sensitivity.[72] Wet spinning is another common method, enabling the fabrication of materials like TPUs,[73] and Ecoflex,[74] which achieve both reversible strain stability and high electrical output. Thermal drawing, a process involving heating and stretching preforms to produce fibers, enhances molecular chain alignment during plastic deformation, thereby improving mechanical strength and triboelectric performance. For instance, Hasan et al. demonstrated the thermal drawing of MXene fibers over tens of meters from preforms.[75] Melt spinning remains a primary method for large-scale production of polyester, nylon, and other synthetic fibers.[49] Additionally, 3D printing technology

View Article Online
DOI: 10.1039/D5EE00144G

offers a simplified route to fabricate MECFs without traditional weaving processes.[76] In summary, traditional spinning is suitable for short fibers, while electrospinning excels in producing nanofibers with high surface areas, albeit at lower efficiency. Wet spinning accommodates non-meltable polymers but incurs higher costs. Thermal drawing enhances fiber properties but requires precise control, and melt spinning dominates large-scale synthetic fiber production, albeit limited to melt-processable materials. 3D printing provides design flexibility but faces constraints in production speed and material selection. Other techniques, including dry solution spinning, reactive spinning, electrochemical spinning, and phase-separation spinning, also contribute to the diverse fabrication approaches for MECFs.

3.3 Signal Response Mechanism

Introducing innovative energy harvesting solutions with advanced sensing technologies can not only enhance the overall performance of devices but also offer new ideas for the design of future smart wearable devices. Wearable sensors typically come in a variety of types. Capacitive sensors rely on the variation in capacitance between two conductors to detect external forces.[77] Piezoresistive sensors measure pressure through changes in resistance that occur in response to applied stress.[78] Piezoelectric sensors exploit the ability of certain crystalline materials to generate electric charges when subjected to mechanical stress.[79] Ferroelectric sensors depend on alterations in the internal polarization state of the material.[80] Thermoelectric sensors are based on the Seebeck effect, converting a temperature difference into an electrical voltage.[81] Electromagnetic sensors involve changes in magnetic flux.[82] Compared to common sensors like capacitive and piezoresistive sensors, MECF's uniqueness in energy harvesting and sensing mechanisms **(Figure 4**a) allows it to respond to dynamic forces with high sensitivity through self-powered methods, offering advantages in energy efficiency and multi-signal output.[83] Thermoelectric and electromagnetic sensors, although self-powered and having flat response curves, are generally less sensitive than triboelectric sensors. With the significant advantage of capturing low-frequency, irregular, and continuous dynamic mechanical characteristic signals, the emerging MECF has excellent performance comparable to piezoelectric and ferroelectric mechanisms.[84-86] Selecting the appropriate sensing mechanism is not an isolated process, but rather requires a comprehensive consideration of various factors, such as the target application field, expected performance metrics, and the complexity of the manufacturing process. Especially in the design of new wearable devices, it is essential to fully balance the relationship between energy efficiency and sensing accuracy, striving to find the optimal balance point.

Due to its hierarchical fiber or textile substrate, MECF naturally possesses a rich surface microstructure and achieves a gradual contact response between fibers from point to surface. (Figure 4b), which can enhance the sensitivity and response speed of pressure sensing. When the dielectric surfaces approach (stage 1), the small amount of charge generated by electrostatic induction will produce a relatively weak signal. The fibers come into contact under continuous pressure (stage 2), resulting in a significant

View Article Online
DOI: 10.1039/D5EE00144G

change in the contact area. Considering the significant change in capacitance, MECF has extremely high sensitivity in this stage. Then, the entire surface is in complete contact under maximized pressure, and the changing contact area leads to sensitivity saturation (stage 3). In contrast, non-textile or other TENGs without specific microstructure designs, likely exhibit less pronounced high sensitivity due to less surface complexity, resulting in a smaller overall response range. Furthermore, as the external force gradually increases, the fibrous network inside the MECF undergoes a series of deformations in a predetermined pattern, thereby effectively converting more mechanical energy into electrical energy. Since the structure of the fibers can be precisely controlled through design and manufacturing processes, their deformation response behavior can be well predicted and adjusted. Therefore, the response characteristics of MECFs have good adjustability by changing the fiber's diameter, length, weaving method, or surface microstructure. In contrast, the planar TENGs have a relatively limited range of adjustment and lower design flexibility. In view of the above-mentioned characteristics, MECF is particularly applicable to those application scenarios that demand high sensitivity, rapid response, a wide frequency range, and self-powered capabilities, such as intelligent wearable devices, human-computer interfaces, health monitoring, and environmental sensing. Other types of sensors, based on their unique working principles and performance characteristics, play significant roles in their respective applicable fields. The design of a multi-linear response can be easily achieved using existing textile processing technologies. This not only reduces production costs but also promotes the possibility of large-scale production. MECF, by virtue of its unique structural design and working mechanism, exhibits excellent performance in multiple performance indicators. Especially in capturing dynamic mechanical signals, it shows great potential and broad application prospects.

View Article Online
DOI: 10.1039/D5EE00144G

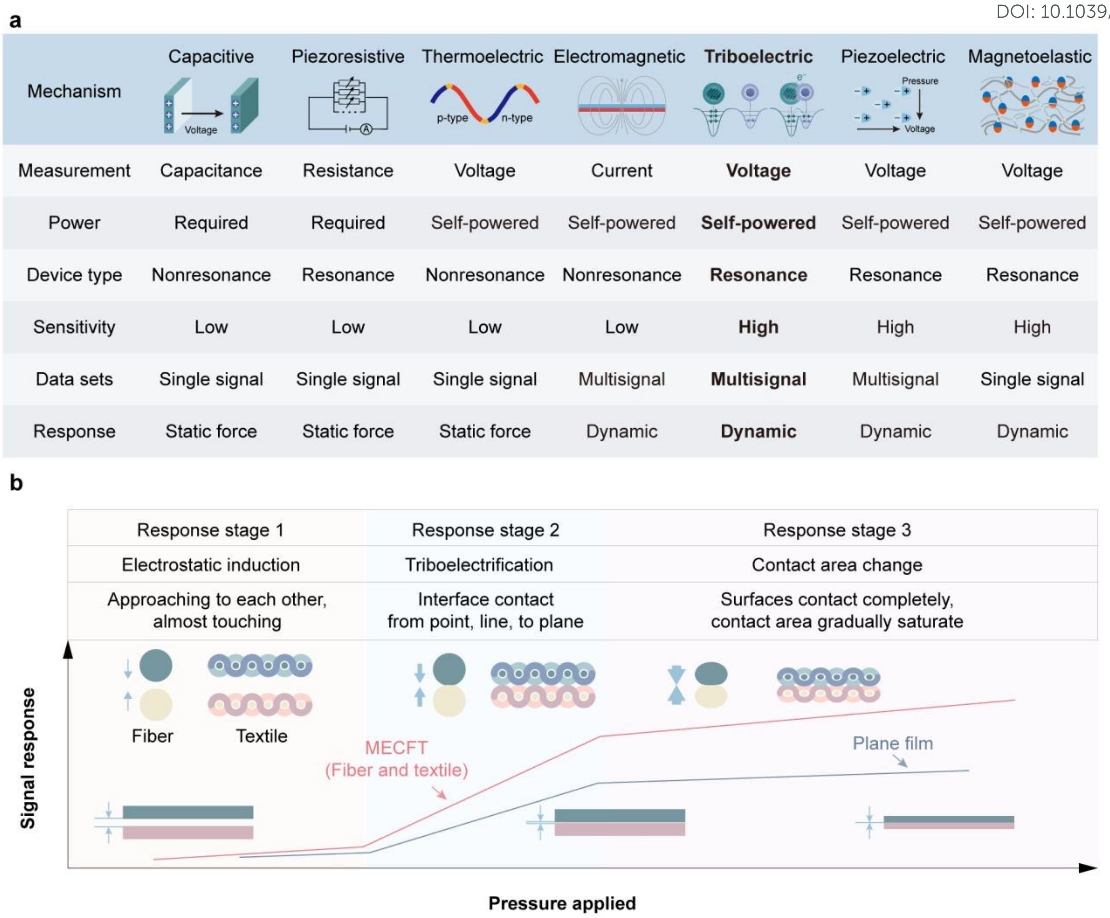

Mechanism	Capacitive	Piezoresistive	Thermoelectric	Electromagnetic	**Triboelectric**	Piezoelectric	Magnetoelastic
Measurement	Capacitance	Resistance	Voltage	Current	**Voltage**	Voltage	Voltage
Power	Required	Required	Self-powered	Self-powered	**Self-powered**	Self-powered	Self-powered
Device type	Nonresonance	Resonance	Nonresonance	Nonresonance	**Resonance**	Resonance	Resonance
Sensitivity	Low	Low	Low	Low	**High**	High	High
Data sets	Single signal	Single signal	Single signal	Multisignal	**Multisignal**	Multisignal	Single signal
Response	Static force	Static force	Static force	Dynamic	**Dynamic**	Dynamic	Dynamic

Figure 4. MECF's multilinear sensitivity response characteristics. a) Comparison of MECFs with other types of sensing mechanism. b) The natural hierarchical microstructure of MECF greatly enhances its sensitivity and response range.

In recent years, the variety of personal wearable electronics has been increasing, with power demand becoming more diverse (**Figure 5**). Fortunately, technological advancements have reduced the average total power consumption of these devices while the energy that MECF can harvest is increasing,[87-91] which exceeds the energy demands of the devices. At the same time, pressure sensitivity S as the core metrics has been promoted significantly in recent years.[72,92-95] Therefore, it is reasonable to believe that MECF has a promising prospect, capable of providing real-time energy supply and signal acquisition functions for popular wearable electronic devices by fully utilizing human motion energy with enough wearable area, thereby achieving a complete closed loop of energy recovery from human's own movements and serving various physiological monitoring and entertainment needs of humans.

View Article Online
DOI: 10.1039/D5EE00144G

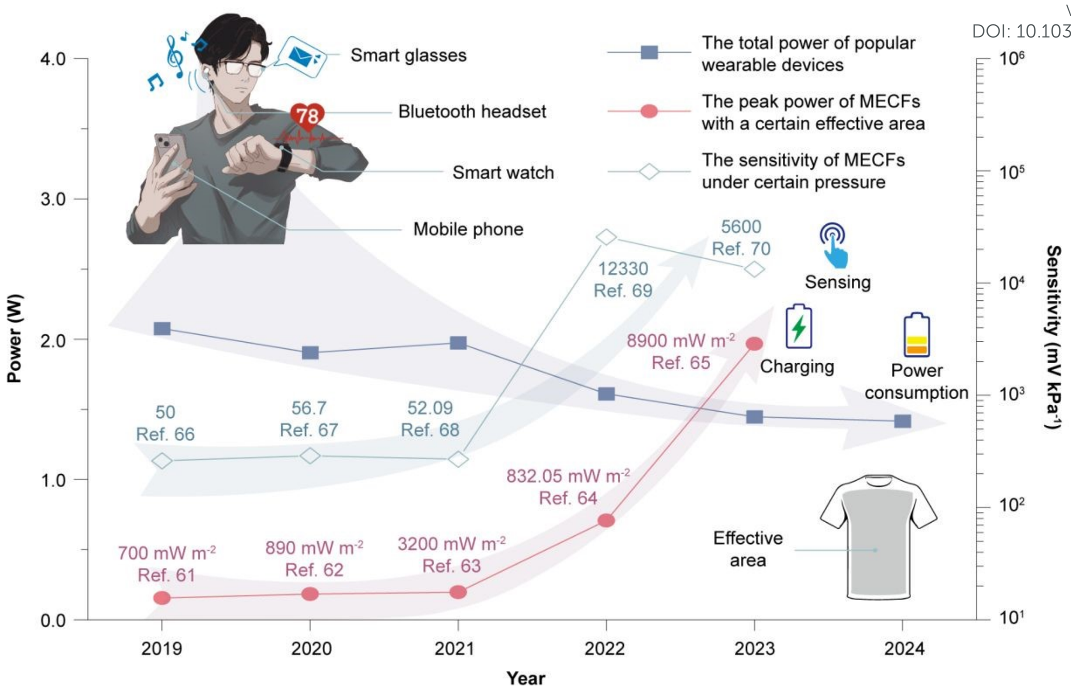

Figure 5. The development history of MECFs in terms of autonomous power output,[87-91] and self-powered sensing.[72,92-95] The gray lines represent the total power of common wearable devices (such as smart glasses, Bluetooth headphones, smartwatches, and mobile phones); the red lines indicate the peak power of MECFs with a certain effective area; and the light blue line shows the pressure response sensitivity of MECFs. The area of MECF is calculated based on approximately 0.22 m^2. The peak power output of MECF has already exceeded the total average power of popular wearable products.

Briefly, in the field of smart health and medical care, MECF serves as an energy supply, signal sensor and implantable medical device,[96-98] by monitoring physiological parameters such as pulse, heart rate, and blood pressure. MECF will replace the large, rigid, and immovable components or sensors in the original system (**Figure 6**). Meanwhile, the applications of MECF in IoT and HMI are transforming the way and offering new possibilities we interact with smart devices.[32,99] The critical role of MECF in security protection has been emphasized,[100] particularly in real-time detection and efficient filtration of hazardous gas or ensuring personal safety under threatens of information, chemicals or disasters. MECF is the irreplaceable fundamental functional component in these application scenarios. This review outlines the latest research progress of MECF in the aforementioned areas, while also highlighting the main challenges currently faced, aiming to provide inspiration and assistance for researchers.

View Article Online
DOI: 10.1039/D5EE00144G

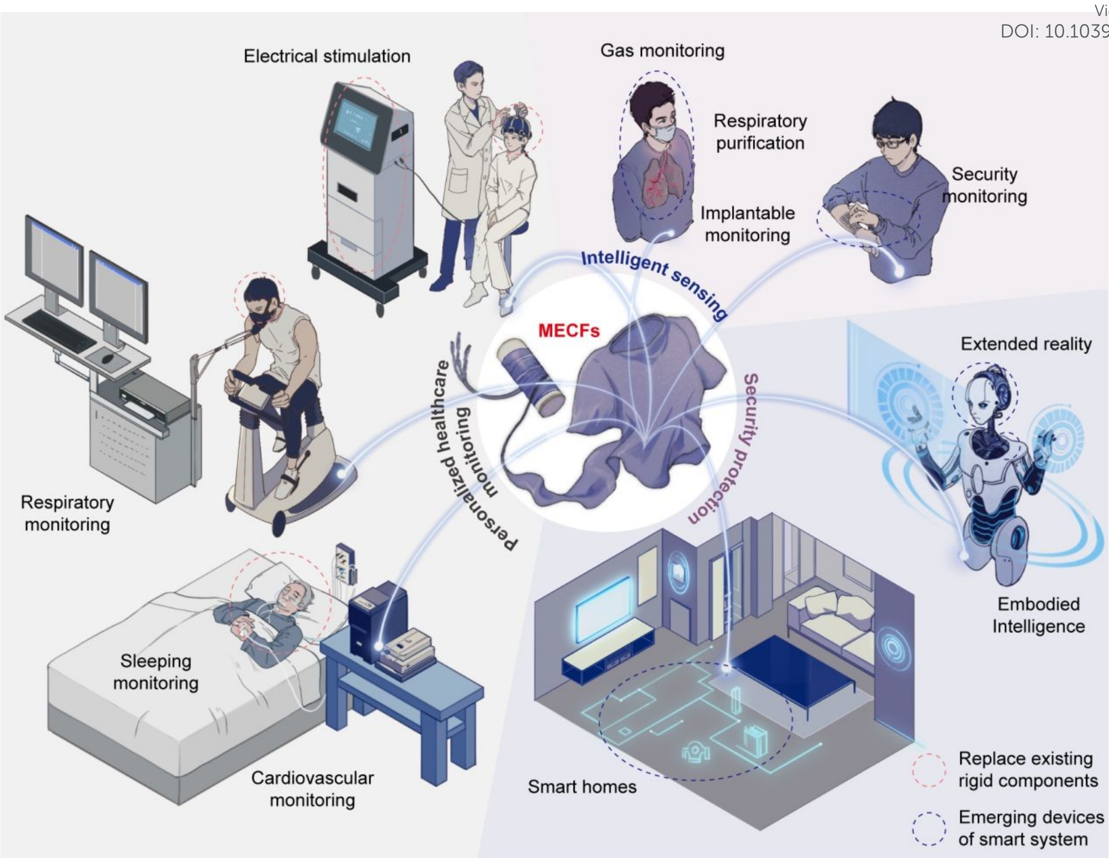

Figure 6. The potential application scenarios for MECFs where they can serve as ubiquitous self-powered wearable sensors. Under this paradigm, MECFs are able to replace the original large and non-portable rigid components and become a basic component in achieving system functionality.

4. Applications for Wisdom Health and Medical Treatment

MECF provides continuous energy support and signal input for wearable and implantable medical equipment. It enables real-time monitoring of human physiological signals including pulse, heart rate, respiratory rate, and plantar pressure, thereby aiding users in promptly assessing their health status and preventing potential diseases. Furthermore, MECF can directly generate electrical stimulation for treatments like wound healing, muscle atrophy recovery, and neural stimulation. Meanwhile, MECF-based smart Internet of medical Things (IoMT) is advancing through the integration of MECF sensors with deep learning algorithms. Such systems enhance the intelligence and automation levels of medical services, providing new means for personalized interventions and disease management.[101]

4.1 Cardiovascular Monitoring

Due to lifestyle changes, urbanization, and an aging population, the risk of cardiovascular disease (CVD) is escalating.[102] Many cardiovascular parameters, derived from pulse waveforms, offer clinically significant information for diagnosing a range of CVD including arrhythmia, atrial septal defect, atherosclerosis, arterial hypertension, and coronary heart disease.[1] Fortunately, modern concepts like "telemedicine," "virtual care," "mobile health," and "E-health" aim to provide continuous, remote, and affordable health monitoring.[103] The adoption of MECF for precisely capturing dynamic pulse information with the device worn on the human body, offers a novel technical approach for real-time monitoring, analysis, and early warning of cardiovascular health conditions.

Pulse monitoring primarily focuses on three key indicators: heart rate (HR), pulse wave velocity (PWV), and blood pressure (BP). PWV serves as an ideal bridge for calculating BP from pulse waves. PWV can be calculated using the Moens-Korteweg equation:

$$PWV = \sqrt{\frac{E \times h}{2 \times \rho \times R}} \tag{3}$$

where E represents the elastic modulus, which quantifies the response of arterial wall to stress-strain; h denotes the arterial thickness, a crucial parameter describing the geometric characteristics of the vascular wall; ρ signifies the blood density, reflecting the ratio of blood mass to volume; and R, the arterial radius, defines the radial dimension of the vascular lumen. Utilizing the Moens-Korteweg equation as a foundation, a linear model can be formulated to correlate BP with PWV:[104]

$$E = E_0 \times e^{\varsigma \times \mathrm{BP}} \tag{4}$$

where ς denotes the material coefficient of the artery, and E_0 represents the value when BP is zero. However, the Moens-Korteweg equation assumes that the arterial wall is isotropic and isochoric with changes in BP, which may not apply to human arteries. Considering this, a relationship between BP and PWV is proposed that does not rely on such assumptions:[105]

$$BP = \alpha PWV^2 + \beta \tag{5}$$

wherein, α and β are determined by the material properties and geometric shape of the artery.

Monitoring CVDs is a crucial aspect of modern healthcare.[106] Traditional monitoring methods often necessitate sophisticated equipment and specialized knowledge. However, the advent of new flexible strain sensor arrays provides a more intelligent solution for monitoring blood pressure and cardiac function parameters.[107,108] A novel flexible strain sensor array, fabricated by carbonized silk georgette (CSG) yarn and laser-cutting nickel fabric (**Figure 7**a–b), can capture pulse wave signals with high accuracy (Figure 7c).[109] Integrated with deep learning algorithms for intelligent monitoring of blood pressure and cardiac function parameters, it remains stable even under conditions such as the Valsalva maneuver (Figure 7d). PWV is a key parameter for CVD prognosis, with an elevated PWV indicating an increased risk of arteriosclerosis and various complications.[110] To accurately measure PWV, a woven and washable triboelectric all-textile sensor array (TATSA) can efficiently generate triboelectricity,[111] achieving a sensitivity of 7.84 V kPa^{-1} and a rapid response time of 20 ms. Based on TATSA, a CVD assessment system is formed (Figure 7e–f) and the PWV is measured to be 13.63 m s^{-1}, which exceeds the average value calculated from the time difference between waveforms and the distance between sensors. BP is one of the most significant factors affecting PWV and is crucial for hypertension diagnosis.[112] Extensive research has focused on measuring blood pressure using MECF.[113] A weaving constructed self-powered pressure sensor (WCSPS) was invented for non-invasive monitoring of human pulse waves and blood pressure with nanowires formed on the PTFE (Figure 7g) to enhance the contact area and sensitivity.[114] It exhibits high sensitivity (45.7 V kPa^{-1}) and an extremely fast response time (< 5 ms). WCSPS is capable of accurately measuring pulse signals from fingertips, wrists, ears, and ankles (Figure 7h), with an error range of 0.87% to 3.65% compared to commercial cuff-based blood pressure monitors.

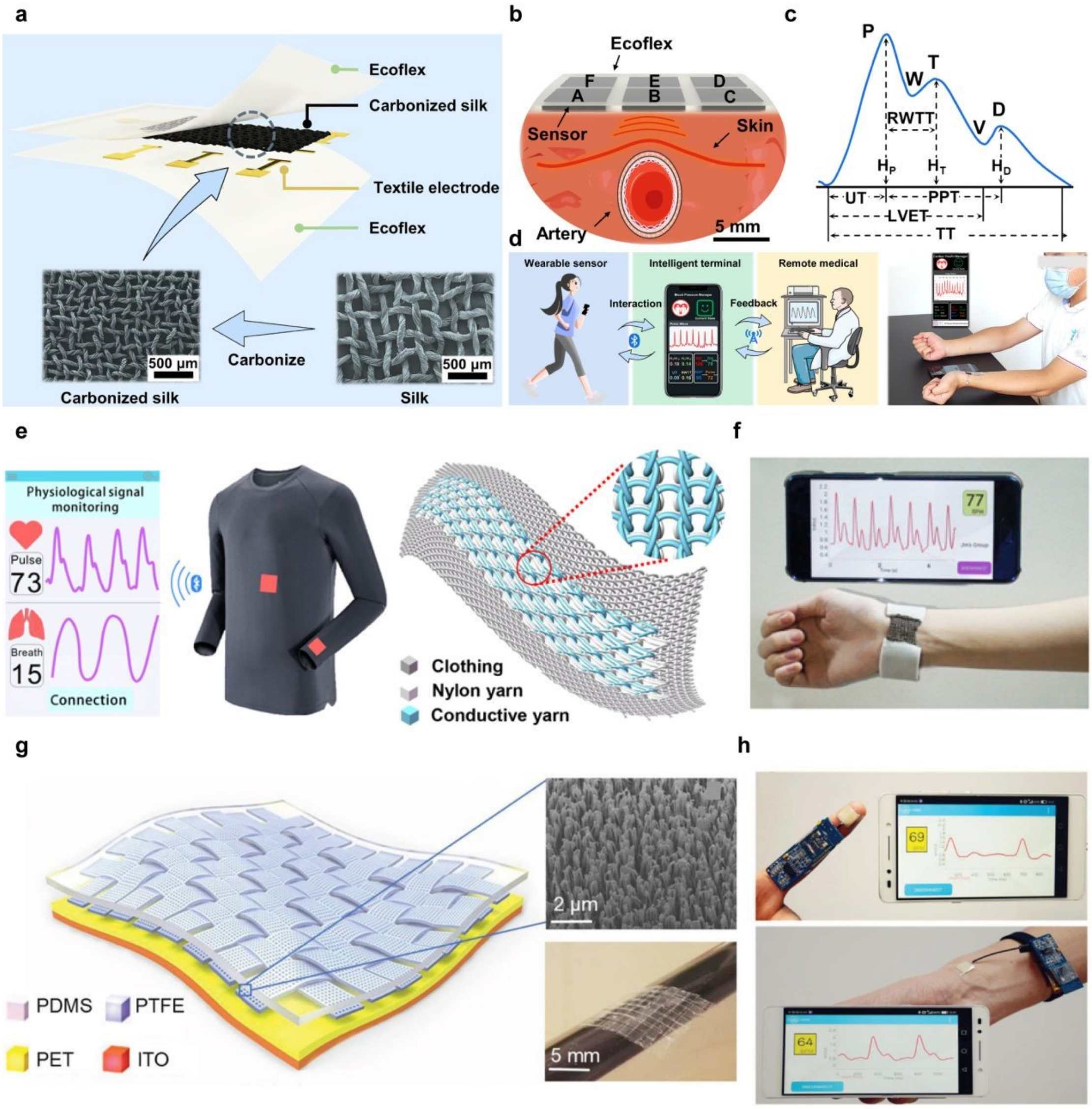

Figure 7. MECF can precisely record pulse waveforms and other CVD information. a) Schematic showing the structure of the sensor array and images of the carbonized silk. b) Schematic illustration of the sensor array collecting pulse. c) Typical radial artery pulse of a healthy person. d) Schematic diagram of the application scenario of the system and Photograph of the health management system a–d) Reproduced with

permission.[109] Copyright 2023, AAAS. e) Schematic diagram of a triboelectric all-fabric sensor array. f) Pulse waveforms are used to calculate brachial-ankle pulse wave velocity. e–f) Reproduced with permission.[111] Copyright 2020, AAAS. g) Schematic representation of a textile triboelectric sensor for h) real-time blood pressure measurement at fingers and wrists. g–h) Reproduced with permission.[114] Copyright 2018, Wiley-VCH.

For pulse detection, MECF exhibits notable advantages over traditional methods, enabling self-powered monitoring without reliance on external power sources. However, the drawbacks should not be overlooked. The electrical output of MECF is relatively low, and its detection accuracy can be influenced by material surface properties and environmental conditions such as humidity and temperature fluctuations, potentially compromising signal quality. Furthermore, MECF monitoring technology is still nascent in analyzing complex physiological signals, and diagnosing specific diseases may require integration with other traditional detection methods.

4.2 Respiratory Monitoring

Respiratory rates serve as a vital sign for monitoring disease progression. Alterations in respiratory rate can predict severe clinical events, such as lung diseases and cardiac arrests.[115] Given the respiratory rate is highly sensitive to various physiological, psychological and environmental stressors, the respiratory rate is superior to other vital signs such as pulse and blood pressure in identifying patients who are in a stable condition and those at risk.[116] Additionally, respiratory monitoring can also significantly contribute to regulating emotions, alleviating stress, and improving sleep quality. In the realm of personalized healthcare, previous respiratory monitors often failed to provide continuous monitoring due to limitations in accuracy and wearability. Consequently, many researchers have turned to novel MECF to monitor human respiratory activities, including respiratory rate, intensity, and duration.[117]

The most common location for MECF to monitor respiratory signals is in front of the mouth.[118] A mask sensor network for respiratory monitoring has been proposed to be mechanically flexible, breathable, moisture resistant and self-powered. The sensor network consists of two layers of PVDF and epoxy resin windings (**Figure 8**a). When combined with the 1D-CNN algorithm, sensor network can achieve real-time and accurate identification of various breathing patterns (Figure 8b). Measuring thoracic gas volume changes is another method to obtain respiratory parameters. An all-yarn-based all-textile sensor (AATS, Figure 8c–d) is capable of accurately capturing and distinguishing abdominal strain signals from three respiratory modes: deep breathing, normal breathing, and rapid breathing.[119] Furthermore, the sensor (size of 40 mm × 30 mm) is combined with a plain-woven belt and fixed to the chest and abdomen. It monitors respiratory activities by sensing volume changes in the thoracic and abdominal cavities during respiration (Figure 8e). Comparative analysis indicated that the differences in respiratory rate between genders were more significant than those between age groups. Many respiratory parameters can also be

View Article Online
DOI: 10.1039/D5EE00144G

monitored on the abdomen. Peng et al. developed breathable, highly sensitive, and self-powered all-nanofiber triboelectric patch (Figure 8f) for real-time respiratory monitoring and diagnosis of obstructive sleep apnea-hypopnea syndrome (OSAHS).[120] The all-nanofiber triboelectric patch features a peak power density of 330 mW m^{-2}, high pressure sensitivity of 0.217 kPa^{-1} and good breathability. Consequently, the all-nanofiber triboelectric patch achieves both energy autonomy and accurate real-time monitoring of subtle respiratory patterns (Figure 8g).

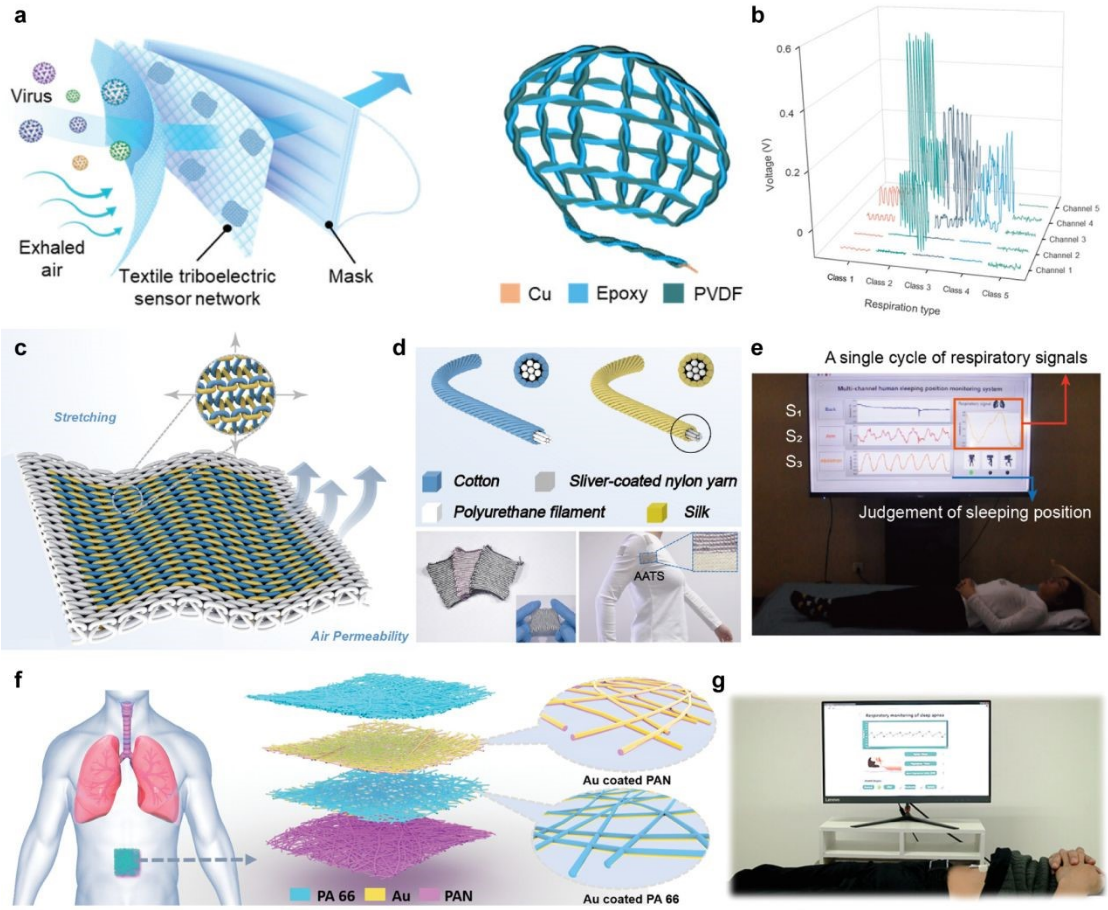

Figure 8. MECF is widely applied in respiratory monitoring. a) Design of an on-mask sensor network and schematic showing the structure of two layers of PVDF and epoxy resin windings. b) Corresponding five-channel output spectra of the collected typical respiratory signals as the input of the 1D-CNN algorithm. a–b) Reproduced with permission.[118] Copyright 2022, Wiley-VCH. c–d) 3D knitted structure of the all-yarn-based all-textile sensor. e) Signal waveforms collected under different conditions. c–e) Reproduced with permission.[119] Copyright 2022, Elsevier. f) Exploded schematic diagram of the obstructive sleep apnea-hypopnea syndrome (OSAHS) structure. g) Photograph of its application in respiratory monitoring scenario. f–g) Reproduced with permission.[120] Copyright 2021, Wiley-VCH.

In comparison to traditional methods such as photoplethysmography and mechanical measurements, MECF for respiratory monitoring exhibits notable

View Article Online
DOI: 10.1039/D5EE00144G

advantages, including high sensitivity, self-powering capabilities, small size for wearability, and the ability to conduct real-time, nuanced monitoring of respiratory patterns. Nevertheless, its clinical application still faces challenges such as durability improvement, signal processing algorithm optimization, personalized adaptation, and data standardization. Future research should concentrate on multi-parameter fusion monitoring, wireless data transmission and analysis, material structure optimization, and clinical validation and application promotion.

4.3 Sleep Monitoring

Sleep, which occupies approximately one-third of a person's lifetime, has garnered significant attention as a crucial indicator for assessing physical and mental health.[121] Its importance lies in 1) facilitating brain function recovery and enhancing cognitive, learning, and memory capabilities;[122,123] 2) achieving physiological balance and repair, strengthening the immune system, and preventing chronic diseases;[124,125] 3) maintaining neuroendocrine homeostasis and preventing stress responses.[126,127] The criteria for evaluating sleep quality encompass sleep onset time, frequency of awakenings, sleep duration, and dream content, which collectively reflects an individual's sleep status. Short sleep onset time, minimal awakenings, sufficient duration (approximately 7–9 hours for adults), and moderate dream activity are indicative of high-quality sleep. Insufficient or excessive sleep can lead to health issues, such as fatigue, cognitive decline, weakened immune function, and psychological distress.

High-quality sleep is inseparable from comfortable bedding. However, many existing sleep monitoring devices are bulky and have exposed wires, leading to high costs and potentially affecting the monitored individual's sleep quality. To address this, a single-layer, ultra-soft, and smart textile consisting of 61 individual sensing units has been developed, which promises to provide comfortable health monitoring during sleep.[128] The authors tested mechanical durability, washing stability, water resistance, etc., to comprehensively evaluate the sensing performance of smart textiles. In addition to the mattress, the pillow is also essential for comfortable sleep. By incorporating a self-powered body-motion sensors with fractal down-like or feather-like structure (**Figure 9**a) into daily bedding items like pillows,[129] a non-intrusive and wireless sleep monitoring solution can be constructed not only distinguish various sleep-related movements including turning over, breathing, snoring, and teeth grinding but also enables wireless transmission of signals to cloud servers or mobile phones for remote early warning of 31 volunteers (Figure 9b), with results nearly equivalent to professional polysomnography (PSG). Another smart pillow design features a 5 × 12 flexible and breathable triboelectric nanogenerator (FB-TENG) pressure sensor array (Figure 9c) for real-time head movement monitoring during sleep,[130] which successfully recorded head movements and real-time head pressure distributions (Figure 9d). Integrating additional functions into the sleep monitoring system is also worth attempting. An all-nanometer fibrous ultra-sensitive pressure and humidity detection array can assess sleep quality. It consists of a multilayer structure made of nanofiber materials with excellent breathability (Figure 9e).[131] The multifunctional sensor accurately records the respiratory rate (RR), heart rate (HR) and assesses sleep environment humidity (Figure 9f). Sleep quality is assessed based on the characteristic RR and HR of different sleep stages as well as the pre-sleep stage (Figure 9g).

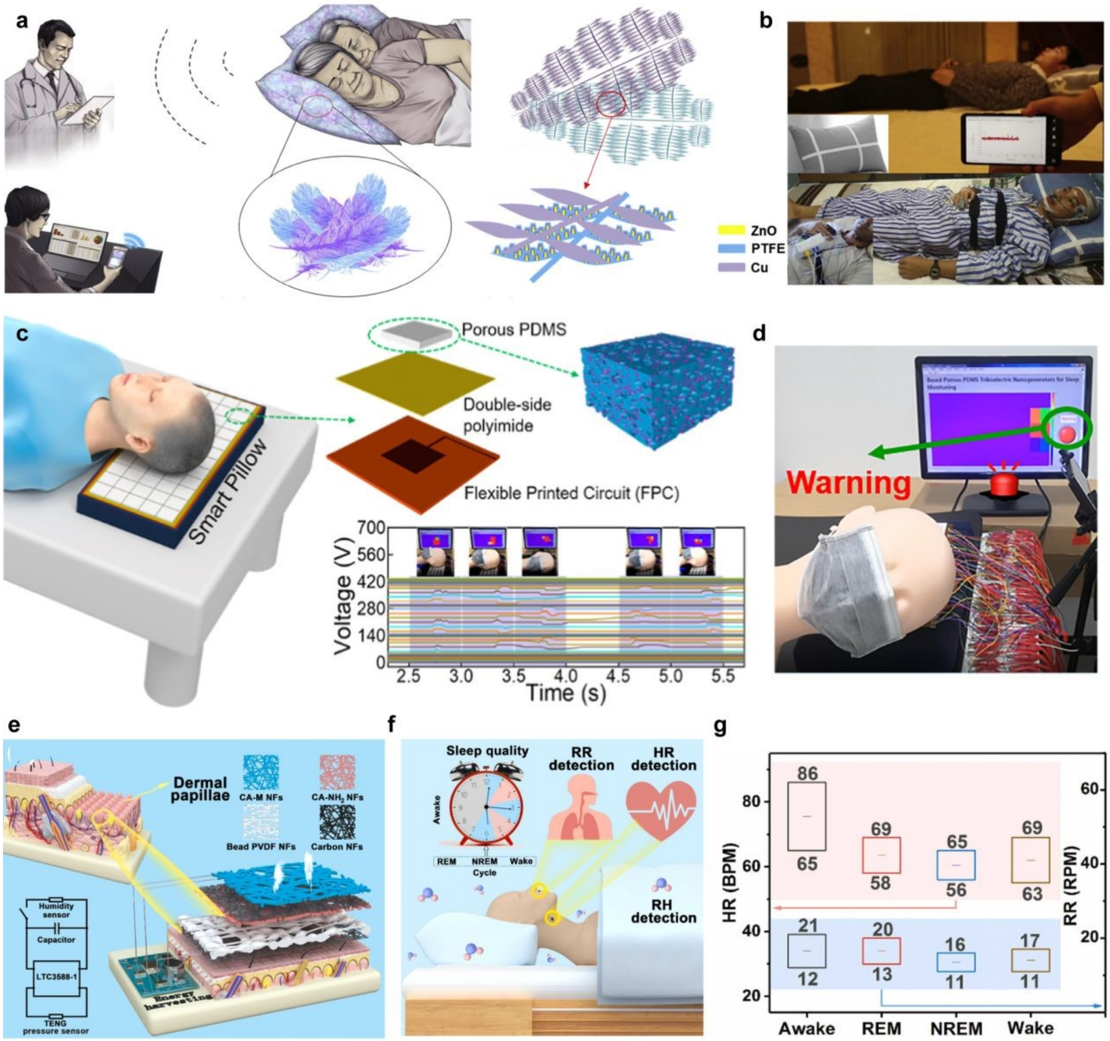

Figure 9. MECF can be easily integrated with sleep accessories. a) Fractal structure of a non-intrusive sleep pillow. b) Recording various sleep behavior signals. a–b) Reproduced with permission.[129] Copyright 2020, Elsevier. c) Schematic diagram of the sensor array integrated into the smart pillow. d) Application example with a mannequin as the subject. c–d) Reproduced with permission.[130] Copyright 2022, American Chemical Society. e) 3D network structure of the all-nanofiber TENG-based multifunctional sensing array. f) Schematic showing how the multifunctional sensor can be used for detecting sleep quality and humidity in the sleep environment. g) RR and HR in different phases of a sleep cycle and during the "awake" phase. e–g) Reproduced with permission.[131] Copyright 2022, Elsevier.

Compared to traditional methods, MECF sleep monitoring technology has the advantages of real-time, non-invasive, low cost, high sensitivity and stability, and wealth of data (e.g., sleep position, pressure distribution), which can be used to accurately assess the sleep quality and conveniently integrated into daily products. Future research should focus on improving sensor sensitivity and resolution to capture subtle sleep changes, developing intelligent algorithms for data analysis, achieving early warning and accurate diagnosis of sleep disorders. Meanwhile, the integration of this technology with other health monitoring technologies (e.g. heart rate, brain wave monitoring) should be explored to establish a more comprehensive physical and mental health monitoring platform.

4.4 Implantable Monitoring

Implantable medical sensors are getting a lot of attention for their ability to convert biochemical, bioelectrical and biomechanical signals to electrical signals for further analysis and monitoring.[132] However, battery usage poses a major challenge due to limited capacity, which cannot sustain the device for long periods, and this will result in subsequent frequent surgeries to replace batteries. The human body harbors a diverse range of energies that can be converted into electrical energy by biocompatible, implantable MECF, providing both power and sensing capabilities.[133-135]

Muscle movements are continuous and frequent, and TENG is capable of not only converting mechanical energy from motion into electrical energy but also monitoring physical properties of muscles with extremely high precision in real time. [136] An organogel/silicone fiber-helical sensor based on a triboelectric nanogenerator (OFS-TENG) with a fibrous structure adheres well to muscles,[137] making it suitable for real-time monitoring of ligament strain when implanted (**Figure 10**a). Myocardial cells proliferation is observed by fluorescence microscopy,[138] and counts of live cardiomyocytes on the sensor after 1, 3, 5 and 7 days show good proliferation tendencies (Figure 10b). Compared to the control group, the inflammation of the tissue surrounding OFS-TENG is milder which demonstrates that OFS-TENG has good biocompatibility (Figure 10c). In addition, planar structures increase the working area than single fiber, which can enhance the output performance of MECF. The implantable passively activated h-TENG (Figure 10d), for example, has good biocompatibility and prevents muscle atrophy by upregulating FGF6 gene expression.[139] The number of proliferating cells increases to five times than the initial count (Figure 10e), which is instrumental in combating muscle atrophy. The h-TENG is placed in the gastrocnemius muscle of mice and performs fluorescent staining (Figure 10f) to analyze the cross-sectional area (CSA) and determined that passive activation of h-TENG better prevented muscle atrophy. MECF can also be used for monitoring other organs or tissues. The bioresorbable triboelectric sensor (BTS) can convert biomechanical movement into electrical signals (Figure 10g).[140] The BTS has excellent antimicrobial properties (99%, Figure 10h), which are maintained throughout the degradation process. Moreover, the BTS has successfully recognized vascular occlusion symptoms in large animals (for example, dogs, Figure 10i). It is promising as an in vivo bioresorbable electronic device for postoperative care applications.

View Article Online
DOI: 10.1039/D5EE00144G

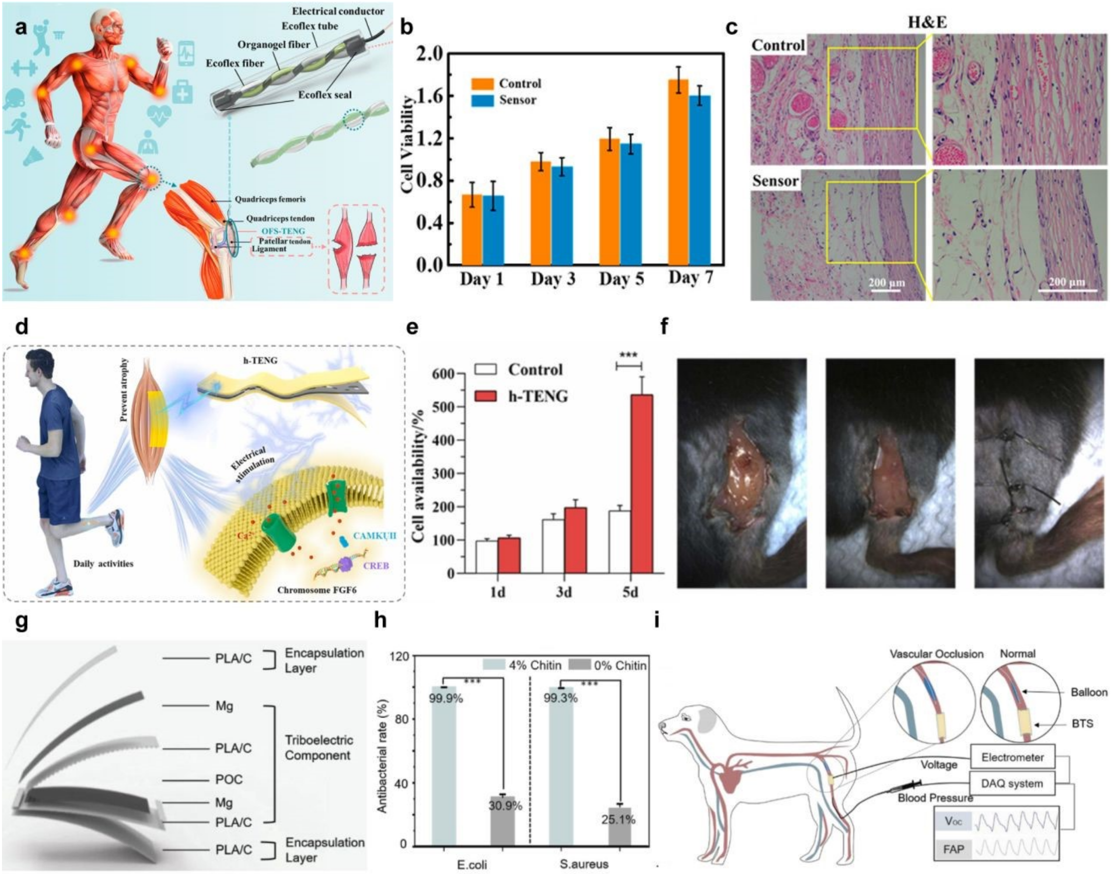

Figure 10. The application of MECF in the field of electrical stimulation therapy. a) Structure and application of the OFS-TENG. b) Cell viability of OFS-TENG for 7 days. c) Photographs of hematoxylin-eosin (H&E) staining of biological tissue implanted in rabbit after 4 weeks. a–c) Reproduced with permission.[137] Copyright 2022, American Chemical Society. d) h-TENG is used to prevent muscle atrophy. e) Cell survival rate compared with the control group. f) h-TENG was implanted into the gastrocnemius muscle of mice. d–f) Reproduced with permission.[139] Copyright 2024, Elsevier. g) BTS structure. h) Sterilization of Escherichia coli and Staphylococcus aureus colonies. i) Application of BTS in dogs. g–i) Reproduced with permission.[140] Copyright 2021, Wiley-VCH.

In summary, MECF has biosensing, therapeutic and power generation capabilities, which enable closed-loop body sensing and healing networks without external power supplies.[141] Implantable MECF will play a crucial role in the prevention, monitoring and treatment of various diseases.[142] However, MECF for implantable sensing still has some drawbacks. Firstly, the optimal implantation location for MECF needs to be further explored to improve biomedical signal sensing. Secondly, more research is needed to clarify the mechanisms of signal generation and the significance of physiological information.[143]

4.5 Electrical Stimulation Therapy

Electrical stimulation therapy is widely applied in pain control, neurological disorders treatment, rehabilitation and muscle function restoration.[144-146] However, conventional electrical stimulation therapy devices are usually bulky, unstable, costly to maintain, and limited in lifespan, which restricts their popularity. MECF has become an ideal solution to these problems due to its small size, low cost, and self-power capability.

Ion introduction technology, which uses tiny voltages and currents, facilitates the penetration of charged drugs into the skin and offers a significant advantage: precise regulation of drug dosages. Integrating the typical ion electroosmotic transdermal drug delivery (TDD) system into a wearable TENG can convert biomechanical motion energy into power for driving and regulating the transdermal drug release process.[147] The organic combination of motion detection and therapeutic functions has been realized (**Figure 11**a). Fluorescence imaging (Figure 10b) and cross-sectional histological pictures (Figure 11c) further validated the conclusion that TENG patch effectively delivered Rhodamine 6G to deeper skin layers. Given the MECF's output ability to act directly on the neuromuscular system, the potential for applying MECF technology as a neuromuscular stimulator is recognized. To enhance the output voltage, an electrical stimulation device based on diode-enhanced textile-based TENG (DT-TENG) is developed which consists of two electrically conductive fabric electrodes: one coated with a nitrile rubber film as a positive triboelectric layer and the other with silicone rubber as a negative triboelectric material.[148] DT-TENG can trigger the tibialis anterior and gastrocnemius muscles, as well as the thicker sciatic nerve of rats, with a higher pulse current output than traditional devices.

MECF also plays an important role in adjunctive treatment. In the field of hair loss treatment, the electrical stimulation method promotes the proliferation of hair follicles through gentle electrical stimulation, regulates the secretion of hair growth factors, and ultimately achieves hair regrowth. The versatile motion-activated and wearable electrical stimulation device (m-ESD) can drive the hair regrowth process via mechanical movement (Figure 11d), effectively overcoming the limitations of conventional electrical stimulation devices.[149] The hair growth length and density of the triboelectric stimulation treatment area were the highest (Figure 11e–f). In arrhythmia treatment, conventional pacemakers, relying on battery power with limited battery life and the need for regular replacement, increase the financial burden on patients and pose additional surgical risks and pain. A novel implantable self-powered symbiotic pacemaker, which consists of an integrated TENG (iTENG), a power management unit and a pacemaker, avoids the above issues.[150] In vivo experiments, the iTENG exhibited an energy output of 0.495 μJ per cardiac cycle, which significantly exceeded the 0.377 μJ required for endocardial pacing. As for the field of limb rehabilitation, processing borophene/Ecoflex nanocomposites into B-TENG allows B-TENG to incorporate into the robotic system as an intelligent keyboard for upper limb medical assistive interfaces or provide real-time feedback for the lower limb's movement patterns.[151] Additionally, it can serve as an extracorporeal electrical stimulation device for continuous wound monitoring and treatment.

View Article Online
DOI: 10.1039/D5EE00144G

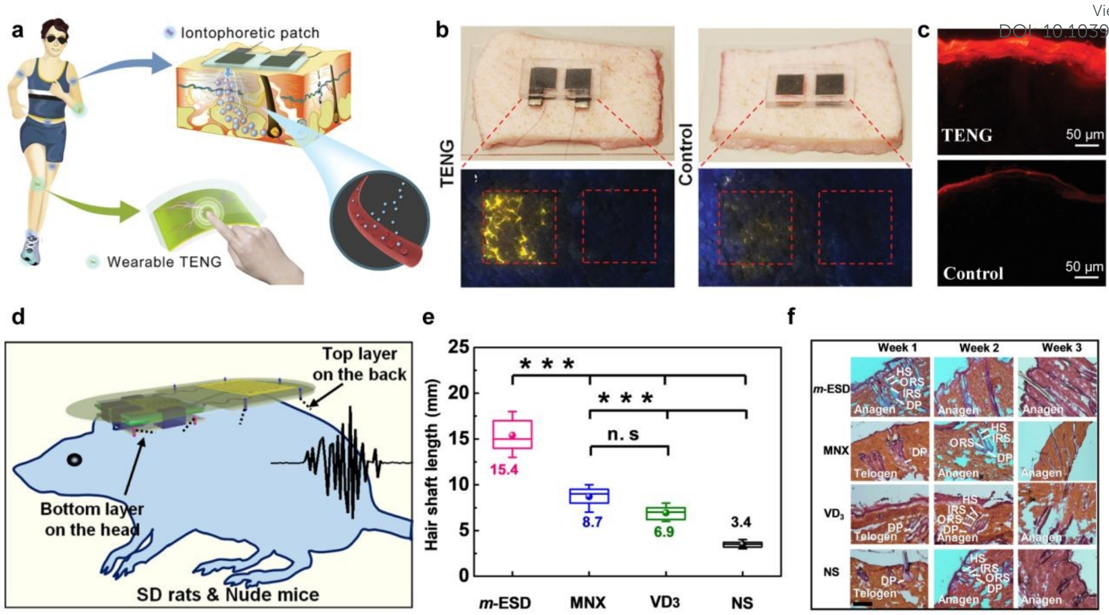

Figure 11. MECF-driven drug delivery and hair growth system. a) Schematic of self-powered iontophoretic TDD system. b) Photographs of a hydrogel drug patch containing Rhodamine 6G on the skin and fluorescent images. c) Histological pictures of fluorescent cross sections of the TENG group and control group. a–c) Reproduced with permission.[147] Copyright 2020, Wiley-VCH. d) Schematic setup of the m-ESD system for hair regeneration. e) Final hair shaft length of rats in the four experimental groups. f) H&E staining of the epidermis under different treatment methods. d–f) Reproduced with permission.[149] Copyright 2019, American Chemical Society.

MECF has revolutionary potential for biomedical applications, enabling a self-sufficient energy supply and reducing reliance on conventional batteries. The electrical signals generated by MECF can be directly utilized in electrical stimulation therapy to promote the repair and regeneration of cells, nerves, tissues and organs. However, MECF technology faces several challenges in practical applications. Firstly, ensuring the biocompatibility of the textile material is essential to prevent biological reactions triggered by the implantable device. Secondly, improving the signal stability of MECF is crucial for the therapeutic effect of electrical stimulation. Lastly, to achieve compatibility with different tissues and organs, further miniaturization and functional integration of MECF are required to minimize the risk of infection and disruption to the patient's daily life.

5. Applications in Internet of Things and Human-Machine Interaction

The field of IoTs and HMI is experiencing a technological revolution.[152] Electronic skin (E-skin) with its bionic tactile perception brings users a more realistic HMI experience. Motion tracking technology enables intelligent responses to user behaviors by capturing human movement.[153] The smart home system incorporates intelligent elements throughout daily life via carpeted flooring, bedding and wireless home devices to enhance living comfort and convenience. Extended reality technology seamlessly connects virtual and reality through gesture control and HMI,

DOI: 10.1039/D5EE00144G

bringing users an immersive new experience.[154] The integration and development of this series of technologies is driving the IoT and HMI towards greater intelligence and humanization.

5.1 Embodied Intelligence

Embodied Intelligence, as a cutting-edge research direction in the field of AI, is pioneering the deep integration of technology and the human body.[155,156] Furthermore, as one of the core technologies of Embodied Intelligence, E-skin achieves accurate capture of external information such as pressure, humidity, temperature, shape, texture, etc. by mimicking the sensing function of biological skin,[157,158] providing a more natural and intuitive way for humans to interact with smart devices.[159,160] In addition, the application of MECF technology provides a scientific basis for athletes' training and competitions, improving their competitive level through real-time monitoring. Collectively, this series of technological breakthroughs promotes the intelligent upgrading of human health, intelligent sports, medical treatment, industry, and other fields.[161]

Integrating the multi-response principle with electrostatic spinning film can expand MECF functionality,[162]and such as the all-fiber tribo-ferroelectric synergistic E-textile with excellent thermal and humidity comfort.[80] Electrostatic spinning technology is commonly used in preparing environmentally friendly fibers.[47,163,164] A hierarchical network structure was constructed, resulting in an E-textile with excellent thermal and humidity comfort (**Figure 12**a) which can serve as a smart insole (Figure 12b) to monitor the gait changes of an individual during exercise. By knitting the sensing fiber, Wei et al. further developed a self-powered multipoint body motion sensing network as an integrated gait recognition system based on an all-textile structure (Figure 12c–d),[165] aiming to detect and differentiate five common pathological gaits (Figure 12e): Parkinsonian gait (PG), scissor gait (SG), mopping gait (MG), gluteus maximus gait (GG) and cross-threshold gait (CG). A multiclass Support vector machine (SVM) with Gaussian kernel function is introduced into the system to achieve 96.7% recognition accuracy classification of five gaits (Figure 12f).

Motion tracking is an important research direction in sports,[166] aiming to accurately monitor athletes' physiological status, technical level, and exercise effect, as well as to enhance the performance and safety of sports equipment.[167,168] MECF can provide scalable solutions for ball sports monitoring.[169] Since different movements apply varying pressure to the MECF, resulting in corresponding voltage signals which can be compared to the standard movements, such as high forehand, high backhand, forehand stroke, backhand stroke, forehand sling and backhand sling, etc. In addition to ball sports, accurately monitoring athletes' physiological status, technical level, and exercise effect in non-ball sports, and improving sports equipment performance and safety, remain major challenges.[170] The running technique monitoring of speed skaters adopts a self-powered portable microstructure TENG,[171] with core components including microstructure PDMS film, fluorinated ethylene propylene (FEP) film, and a lithium chloride-polyacrylamide (LiCl-PAAM) hydrogel. This portable microstructure TENG can be easily attached to an athlete's body to accurately collect technical motion information such as movement structure, bending angle and frequency.

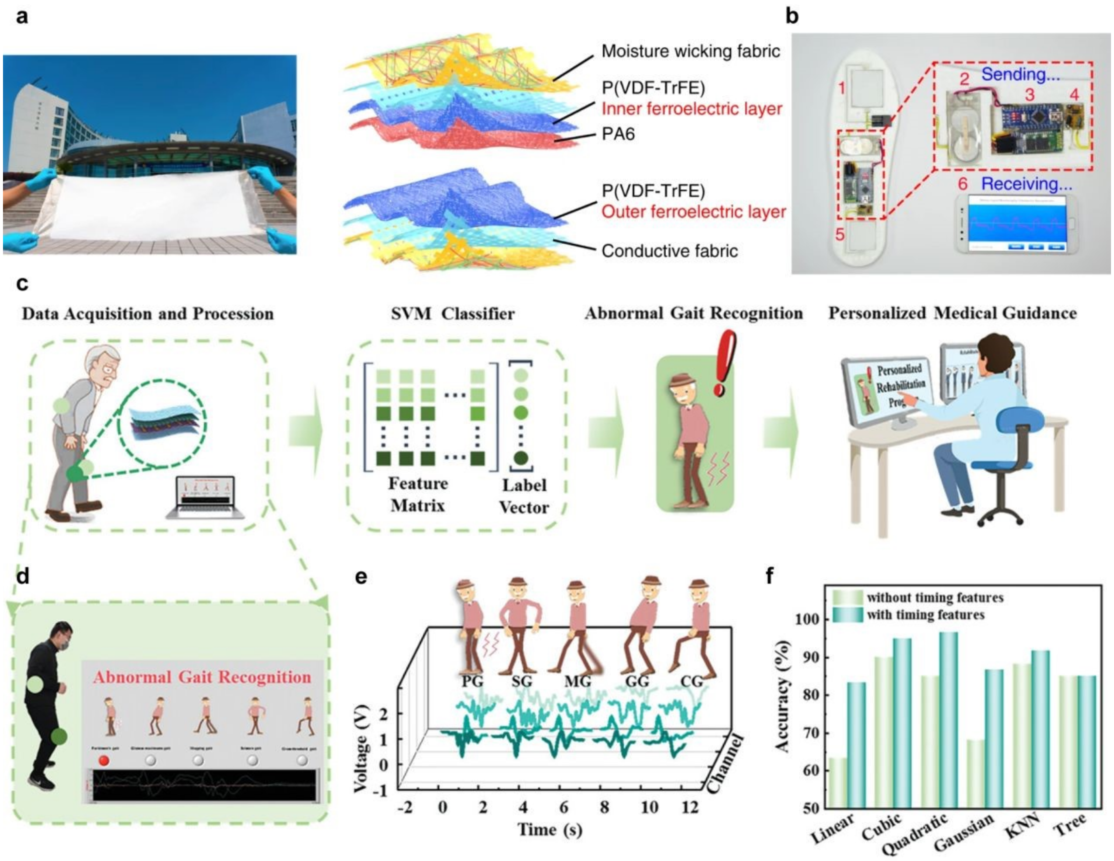

Figure 12. MECF-based E-skin for somatic motion monitoring. a) The physical and structural diagram of an all-fiber contact-separation mode tribo-ferroelectric synergistic E-textile (105 × 35 cm). b) Hardware connection of self-powered gesture monitoring system placed on a 3D-printed insole. a–b) Reproduced with permission.[80] Copyright 2019, Springer Nature. c) and d) Schematic diagram of a real-time gait monitoring system for biological gait recognition and assisted rehabilitation training. e) Maps and typical multichannel sensing signals for five deformed gaits. f) Comparison of the classification accuracy of different machine learning algorithms. c–f) Reproduced with permission.[165] Copyright 2023, Wiley-VCH.

The introduction of MECF not only improves real-time tracking and accuracy in sports tracking but also provides strong technical support for the development of intelligent sports. However, technical difficulties persist in improving sensor sensitivity and long-term stability, as well as in developing more cost-effective energy conversion and data processing technologies. In the future, MECF is expected to further enhance sports training and competition through sport-specific sensor design and data analysis methods.

5.2 Smart Homes

With the rapid development of information technology, smart homes have

View Article Online
DOI: 10.1039/D5EE00144G

gradually become a significant aspect of societal progress.[172] In a smart home environment that is equipped with a highly advanced automation system, people can control household appliances such as air conditioners and lamps through voice and other methods, establishing interactions with them, and achieving a high level of home automation. Voice control is convenient when hands are wet, busy, or otherwise occupied, and has a high degree of individual differentiation,[173,174] so it can be an effective medium for contactless and remote monitoring and interaction/control in smart homes.[37]

At the same time, in the field of smart homes, many daily items are essentially textiles, such as carpets, bedding, curtains, and sofas. The development of MECFs provides a foundation for expanding the functionalities of these traditional textiles. In a smart home environment, textiles like carpets occupy the largest area in the home and are one of the most frequently touched interfaces in our daily activities. Smart flooring requires not only the implantation of numerous sensors, but also an external power supply for data acquisition, signal conversion, and transmission. To solve the current problem of high floor cost, Shi et al. developed a floor monitoring system and proposed a triboelectric coding pad (Figure 13a).[175] The output from the human stepping motion has an opposite polarity, so the overlap results in significant peak deviation. To eliminate this adverse effect, the authors implemented an interval parallel scheme where adjacent mats are connected to different electrode groups. The interval parallel scheme, along with the output, shows more reliable and ideal characteristics (Figure 13b). Another self-powered triboelectric deep learning-enabled smart mats (DLES-mats, i.e., floor mats) is proposed.[176] DLES-mat (Figure 13c) is manufactured using low-cost and highly scalable screen-printing technology with a unique “identity” electrode pattern (Figure 13d–e) that enables sensing user position and identification to turn on the corridor lights for illumination.

MECFs not only bring the possibility of intelligence to traditional textiles but also offer new insights into the overall optimization of smart home systems. We present these application scenarios precisely to highlight the great potential of electromechanical conversion fibers in smart home textiles. However, MECFs in smart homes still face multiple challenges, including data privacy protection, device compatibility and system integration. Future research needs to focus on how to realize seamless interfacing and cooperative work between different devices while safeguarding user privacy.[177] The smart home technology industry is expected to realize energy saving and overall lifestyle improvement by addressing the challenges currently faced.

DOI: 10.1039/D5EE00144G

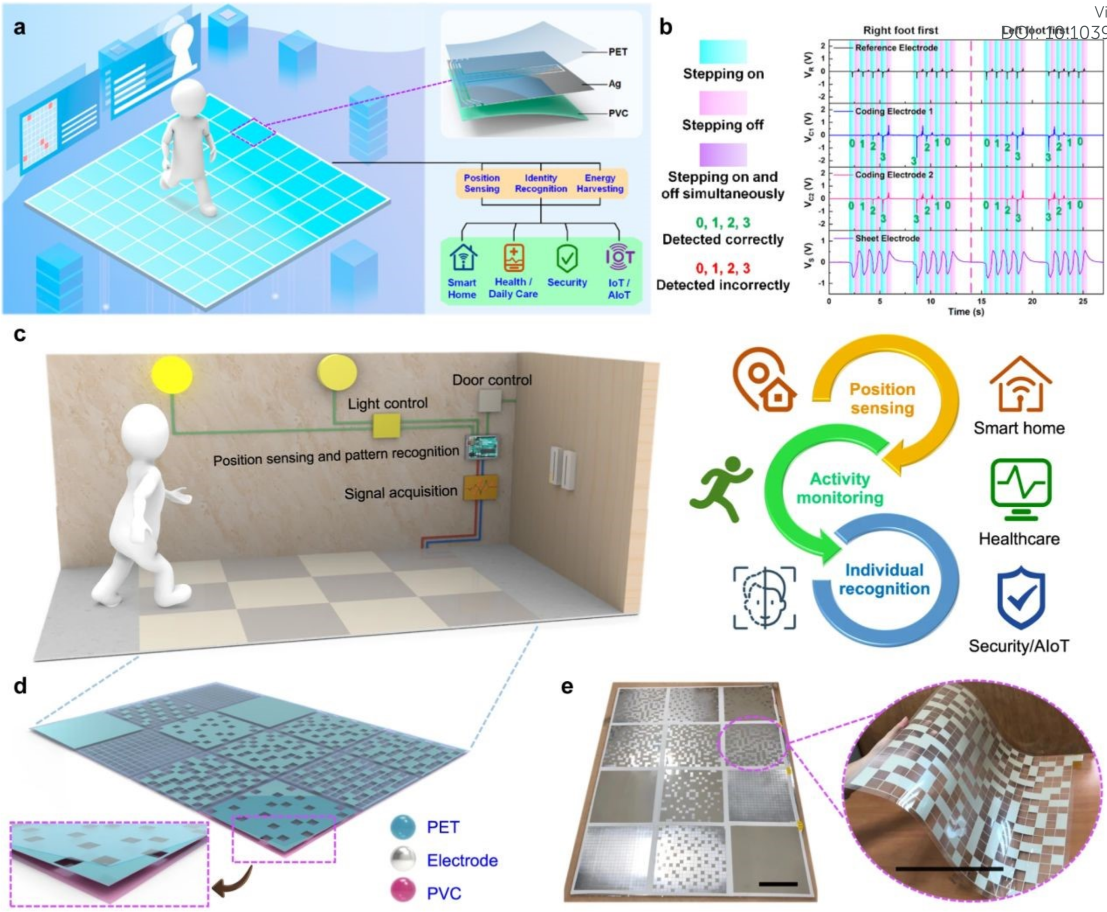

Figure 13. MECF's applications of carpet flooring, bedding, and wireless homes in smart homes. a) Robust and intelligent floor monitoring system. b) The interval parallel scheme. a–b) Reproduced with permission.[175] Copyright 2021, American Chemical Society. c) Conceptual diagram of the intelligent floor monitoring system. d) An assembled triboelectric DLES-mat array in a 3 × 4 arrangement. e) Digital photographs of a mat array and a single mat with 40% electrode coverage. c–e) Reproduced with permission.[176] Copyright 2020, Springer Nature.

5.3 Extended Reality

Virtual reality (VR) technology bridges the gap between virtual life and the real world. A variety of methods have been applied to VR interaction, such as visual imaging-based methods and inertial sensor-based wearable devices. However, these methods have significant drawbacks: digital imaging systems used for body motion interaction are typically composed of fixed, expensive, and bulky equipment, which makes them inconvenient to reposition and unsuitable for tracking long-range and moving objects.[161] To avoid these drawbacks and provide a better user experience to users, MECF-based sensors have received attention for their significant advantages in terms of wearability and adaptability.[178,179]

Gesture-based wearable MECF sensors are now used as the most popular interactive way in VR or communication assistance.[180] The glove holds great promise for detecting the multi-degree of freedom hands' movement. Combining convenience, intuitiveness, and low cost of the glove platform with the dynamic sensing effect and

View Article Online
DOI: 10.1039/D5EE00144G

self-powered capability of MECF technology is extremely promising. A sensing system with patterned electrode tactile TENG (T-TENG) detects soft gripper sliding, contact position, and clamping mode, and uses a length TENG (L-TENG) to measure the bending angle of the soft actuator.[181] Hence, T-TENG sensors and L-TENG sensors form a glove-based human-machine interface for real-time control of manipulators. Wen et al. developed a sign language recognition and communication system consisting of an integrated TENG glove, an AI module, and a VR interactive interface (**Figure 14**a).[182] The recognition results are projected into virtual space as intelligible speech or text (Figure 14b), to promote accessible communication between signers and non-signers. The system successfully recognized 50 words and 20 sentences (Figure 14c) and can identify new sentences it has not encountered before. Beyond hand gestures, other body movements can also translate the user actions as input commands, providing a natural way to facilitate HMI. Smart socks with triboelectric sensing function (Figure 14d) can provide more comprehensive long-term monitoring of the user's physical status.[183] Pressure sensors are placed in different areas (Figure 14e) so smart socks can gather information from foot movements for more sophisticated gait analysis. The good stability and adaptability of smart socks make them suitable as a control interface for VR fitness game (Figure 14f). At the same time, monitoring changes in muscle shape due to muscle contraction is valuable for exercise monitoring.[184] A non-invasive muscle sensing wearable device has been proposed, which is combined with machine learning to enable motion-control based body sensation to interact with avatars.[185] The device utilizes a flexible 16-channel pressure sensor array to simultaneously detect muscle mechanical activity, including shape changes and vibration, which provides an alternative to traditional rigid inertial measurement units and EMG-based methods for accurate real-time control of avatars in virtual space.

Human emotions are considered a key factor in HMI. However, recognizing emotional information is very challenging due to its abstract and fuzzy nature. Lee et al. propose a human emotion recognition system which is equipped with bi-directional triboelectric strain and vibration sensors using a personalized skin integrated facial interface (PSiFI) to recognize complex emotional states (Figure 14g).[186] Signals from the strain sensing unit exhibited distinct patterns for facial expressions, such as happiness, surprise, disgust, anger, and sadness (Figure 14h). Additionally, a digital concierge that classifies emotional speech classifying system in VR environment was demonstrated (Figure 14i).

View Article Online
DOI: 10.1039/D5EE00144G

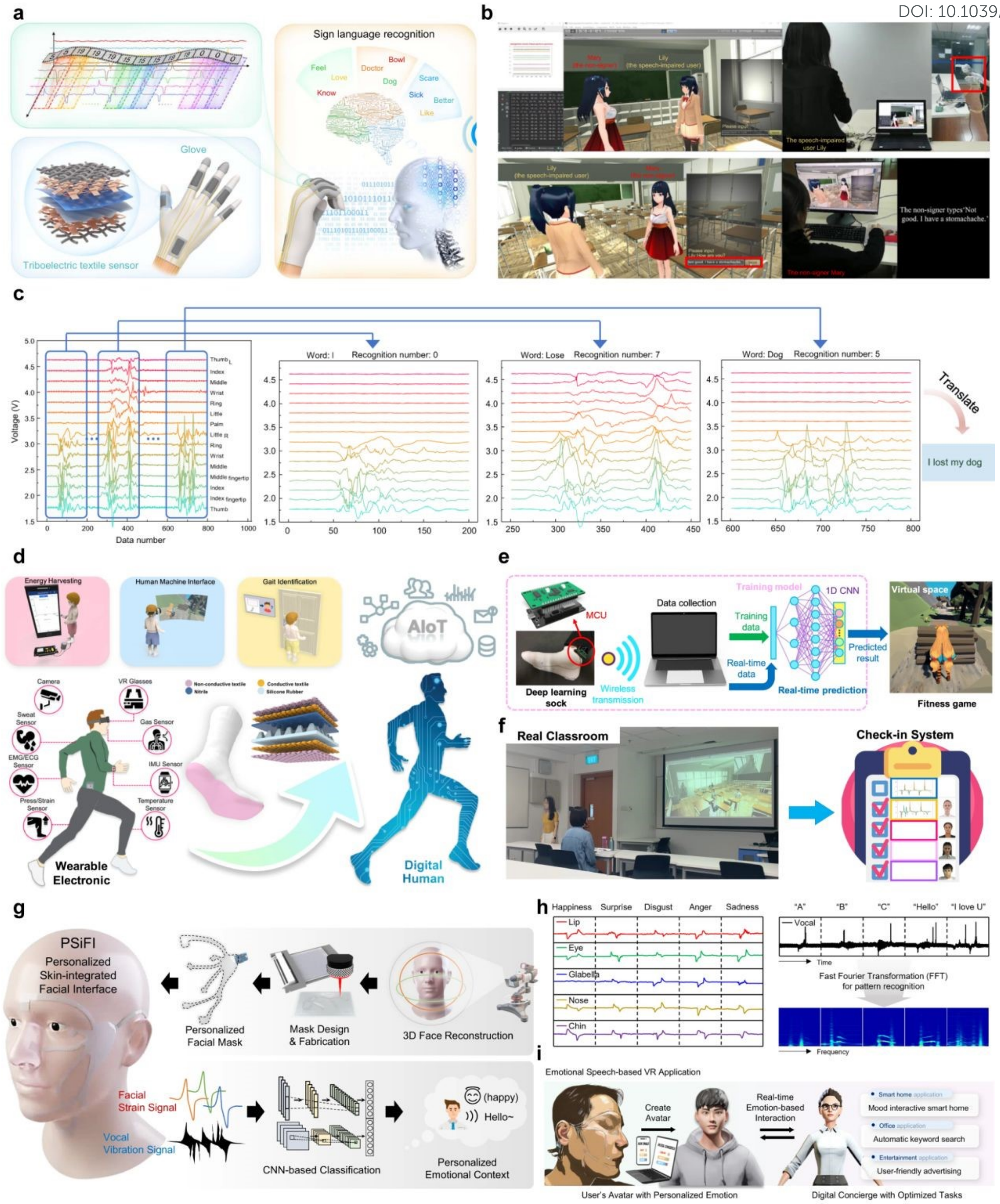

Figure 14. MECF serves as an important medium for HMI and extended reality. a) Schematic diagram of the sign language recognition and communication system. b) Dialogue process between non-signing users with language barriers in VR interface. c) Process of recognizing three new sentences not previously learnt. a–c) Reproduced with permission.[182] Copyright 2021, Springer Nature. d) Applications for smart socks. e) Three-channel output characteristics. f) Real-time display in VR. d–f) Reproduced with permission.[183] Copyright 2020, Springer Nature. g) Schematic of PSiFI. h) Facial strain and vocal fold vibration signals from skin-integrated interfaces. i) Schematic representation of how users interact with digital concierge services. g–i) Reproduced with permission.[186] Copyright 2024, Springer Nature.

In summary, in the era of 5G and IoT, MECF-based wearable sensors hold significant potential for extended reality applications.[187] However, MECF needs to further improve the accuracy and robustness of sensors, as well as develop more advanced algorithms to process complex multimodal data for more accurate emotion recognition and action interpretation. Future research directions should focus on improving the sensitivity of MECF, reducing power consumption, and enhancing the practicality in various scenarios, including medical rehabilitation training to realize truly natural interaction and immersive virtual experiences.

6. Application for Environmental Monitoring and Personal Protection

MECF plays a key role in environmental monitoring and personal protection, serving as a key technology for safeguarding human health, safety and ecological quality.[188] It powers hazardous substance detection equipment for real-time monitoring and early warning and drives personal protective equipment for efficient dust removal and filtration by converting human activity energy into electrical energy. MECF aims to comprehensively identify, assess and control environmental risks through scientific methods and technological means, thereby contributing to a safer and healthier living environment.

6.1 Hazardous Gas Monitoring

The accumulation of such hazardous substances has a serious impact on human health, so the detection of hazardous substances is critical for environmental monitoring, protection, and safeguarding human health. The self-powered capability of MECF provides a novel solution for hazardous material detection.

High concentrations of nitrogen dioxide (NO_2) in the atmosphere contribute to the formation of photochemical smog and acid rain. Low concentrations of NO_2 can also threaten human health. Prolonged exposure to NO_2 gas can cause lung diseases, respiratory illnesses and reduced immunity. Therefore, an efficient wind-driven self-powered NO_2 detection platform (**Figure 15**a) was developed,[189] which exhibited significant voltage response at different NO_2 concentrations (0.5–50 ppm) (Figure 15b). The voltage response at 50 ppm NO_2 ($\Delta U_s/U_{sa}$ = 510%) even exceeded that of the resistive sensor ($\Delta R/R_a$ = 0.33) by a factor of 15. To fully utilize the wind in all directions, four PVA/Ag-based TENGs were integrated into the platform (Figure 15c) to provide a stable power supply. In addition to utilizing the energy of airflows, harvesting the body movements energy is more universally applicable. A novel MXene/TiO_2/C-NFs heterojunction-based sensory assembly based on cellulose nanofibers (C-NFs) is sewn on the socks to detect NH_3 (Figure 15d), exhibiting excellent reproducibility, high selectivity, sensitivity to NH_3 (1–100 ppm) at room temperature, with a fast response/recovery time (76 s/62 s) (Figure 15e).[190] Optical detection methods are equally important as chemical detection. A wearable system integrates a textile-triboelectric nanogenerator (T-TENG) as power source and a Fabry–Pérot filter (FPF) serving for gas detection was reported (Figure 15f).[191] Experiments revealed that the accuracy of reconstructing acetone spectra was comparable to a commercial power supply (Figure 15g-h), demonstrating the

View Article Online
DOI: 10.1039/D5EE00144G

feasibility of using TENG as a power source, with a mean-square error of only 9.58×10^{-3} for reconstructed spectra. In many applications, such as food storage, industrial production, and environmental monitoring, the accurate detection of ethanol is essential for safety, quality control, and environmental protection. However, traditional detection technologies often suffer from limitations in sensitivity, response speed, and stability, hardly meeting the demand for real-time, high-precision detection of low concentrations of ethanol gases. To expand the application scenarios of self-powered ethanol monitoring systems, a tire-driven triboelectric-electromagnetic hybrid nanogenerator (HNG) for self-powered gas monitoring has been developed.[192] A $Ti_3C_2T_x$ MXene/Ag-based sensor driven by HNG can be applied to detect ethanol. The high response of the self-powered ethanol sensor ($\Delta U_{ab}/U_{ab(gas)}$ = 204%@100 ppm) is 24.5 times greater than that of a resistive sensor ($\Delta R/R_a$ = 8.3%). Humidity effects can be minimized by drying pretreatment or humidity compensation of the gas samples.

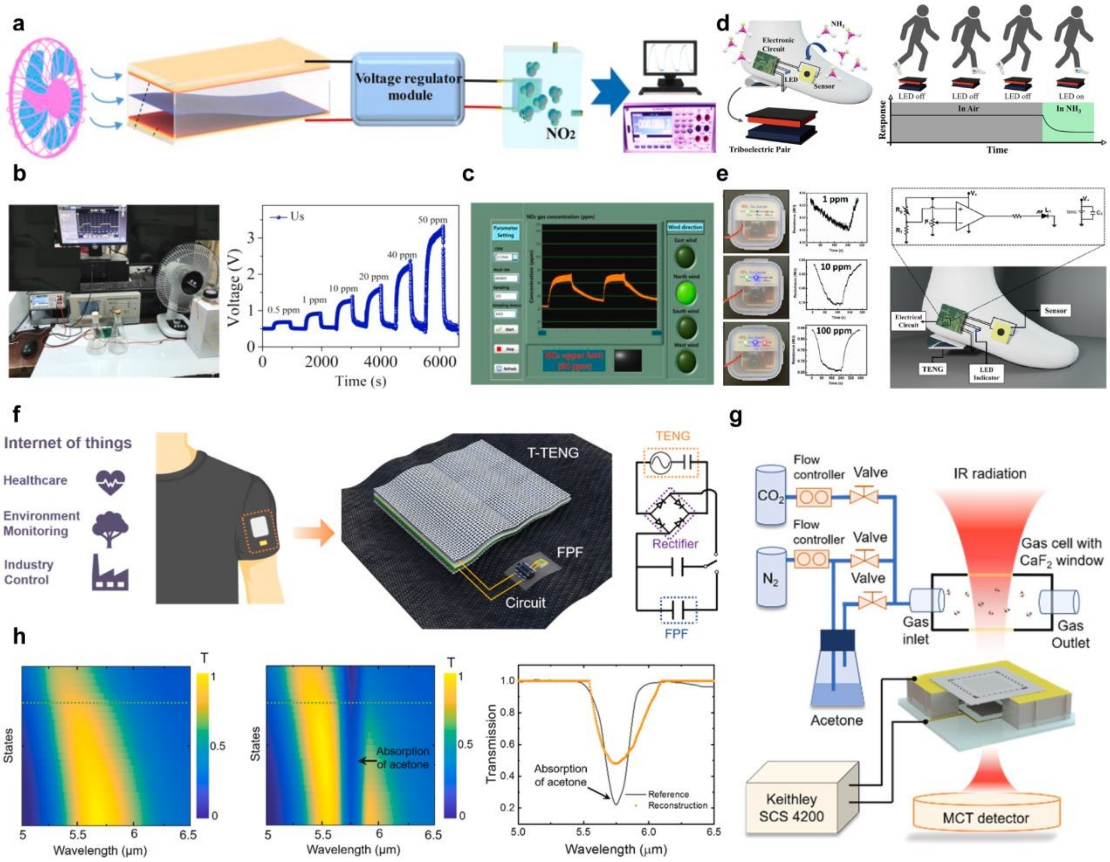

Figure 15. MECF-driven gas detection system. a) Schematic illustration of self-powered NO_2 sensor driven by TENG. b) The wind-driven self-powered NO_2 detection platform. c) The voltage of Us under different concentrations of NO_2. a–c) Reproduced with permission.[189]. d) Schematic illustration of a smart shoe insole. e) Photographs of the LED response in 1 ppm of NH_3, 10 ppm of NH_3, and 100 ppm of NH_3. d–e) Reproduced with permission.[190] Copyright 2022, American Chemical Society. f) Envisioned wearable optical miniaturized spectrometer using TENG enabled tunable FPF, and its equivalent circuit diagram. g) Testing setup including

View Article Online
DOI: 10.1039/D5EE00144G

gas supply system. h) FPF spectral analysis for acetone detection. f–h) Reproduced with permission.[191] Copyright 2021, Elsevier.

Despite significant progress in the detection of harmful gas components, there are still two important issues that need to be addressed. The first one is that environmental adaptability for TENG's accuracy may be compromised by environmental conditions such as humidity and temperature. The second is cross-sensitivity, as TENG could react to non-target gases, causing cross-sensitivity problems. This will rely on further structural design and modification methods such as chemical functional group grafting to address.

6.2 Air Pollution Control

Nowadays, air pollution has become a significant issue affecting people's daily lives and social development.[193] Among various pollutants, airborne particulate matter (PM) is considered one of the greatest danger, severely degrading air quality, public health, and ecosystems.[162] At present, the common way to prevent air pollution is to wear masks, but conventional masks have a low filtration effect and a relatively short service life. Additionally, discarded masks contribute to environmental pollution. Therefore, there is an urgent need for a sustainable mask to replace traditional masks and reduce environmental damage.

Masks based on MECF can simultaneously combine two of the most common technologies for PM removal, namely fiber filtration and electrostatic precipitation (ESP),[194,195] corresponding to the vast adsorption area of textile fibers and the high-voltage electric field generated by triboelectricity.[196] Additionally, MECF enables the creation of masks with various functions, including antiviral protection.[197] Replacing the filter layer of commercial masks to improve surgical masks' filtering efficiency for nano to micro-sized particles is an intuitive choice, so an enhanced triboelectric mixed nano/microfiber air filter is proposed. This filter is constructed by an electrospun nanofibrous network and poly (3,4-ethylenedioxythiophene: poly (styrenesulfonate) (PEDOT:PSS) coated polypropylene (PP), as shown in **Figure 16**a.[198] The surface topography of PP/polyacrylonitrile (PAN) after 4 hours of testing shows visible particle clumping, indicating the filter's efficiency at capturing airborne particles (Figure 16b). Meanwhile, the hybrid filter exhibits a 100% sterilization effect (Figure 16c). Maximizing the service life is also an important means of improving user experience and reducing usage costs. Therefore, a self-charging air filter (SAF), composed of a PVDF nanofiber membrane and a nylon layer, is assembled into a commercial mask to withstand the test of reliability from prolonged use (Figure 16d–e).[199] Four subjects are invited to wear masks for 10 hours per day for three consecutive days for a total of 30 hours. After 60 hours of testing (including 30 hours of wear), the mask's filtration efficiency remained as high as 95.8% and the respiratory resistance increased only from 85.1 Pa to 86.4 Pa (Figure 16f). In the context of sustainable development, developing biodegradable materials is just as important as enhancing filtration performance. Utilizing unique organic-inorganic hybrid nanocomposite materials, such as PBAT@CTAB-MMT, can achieve various

DOI: 10.1039/D5EE00144G

functions, including biodegradability, antibacterial, and antiviral properties.[200] The PBAT@CTAB-MMT nanofibrous membrane (NFM) consists of polybutylene adipate (PBAT) matrix blended with cetyltrimethylammonium bromide (CTAB) and montmorillonite (MMT) clay (Figure 16g). PBAT@CTAB-MMT NFM showed a high inhibition rate of 99.8% compared to the control (Figure 16h), indicating successful sterilization. In terms of the removal efficiency of NaCl NPs (Figure 16i), the filtration efficiency of the frictionally charged PBAT@CTAB-MMT NFM filter was approximately12% higher than that of the uncharged filter (98.27% to 85.56%).

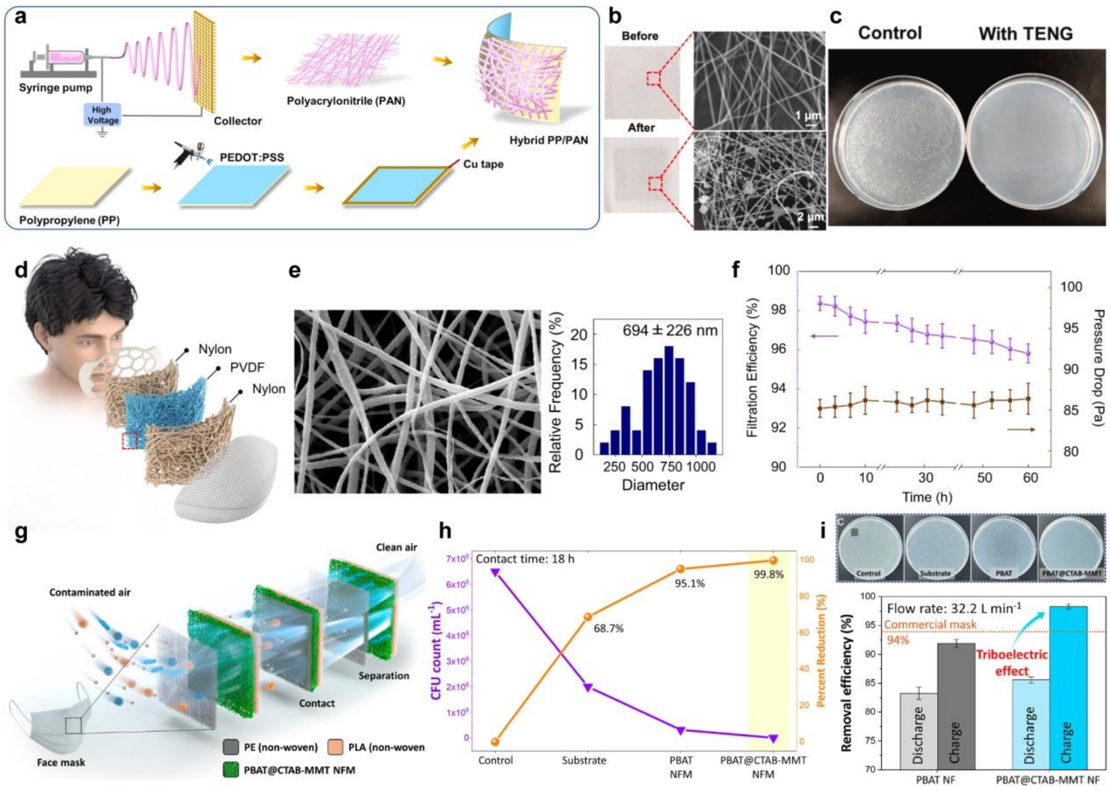

Figure 16. MECF for air pollution control. a) Manufacturing process for hybrid air filters. b) Photographs and SEM images before and after long-term stability test. c) Photographs of agar plates of the sterilization effect. a–c) Reproduced with permission.[198] Copyright 2021, Elsevier. d) Schematic diagram of a self-charging air filtration mask. e) Morphology of nanofibers. f) Durability evaluation of filtration efficiency and pressure drop. d–f) Reproduced with permission.[199] Copyright 2022, Springer Nature. g) Schematic of the structure and performance of the multifunctional mask filter. h) Determination of antimicrobial resistance by agar plate counting technique. i) Evaluation of filtration efficiency. g–i) Reproduced with permission.[200] Copyright 2022, American Chemical Society.

In conclusion, the application of MECF-based air filters in masks shows great potential to effectively remove airborne particles, bacteria and viruses. Furthermore, this technology extends service life and offers sterilization effects.[201] However, several challenges remain to be addressed. For instance, improving filter efficiency

DOI: 10.1039/D5EE00144G

and ensuring mask comfort and breathability are key. In the future, researchers need to explore biodegradable materials to further improve the filtration efficiency and comfort of masks. In addition, the recycling and disposal of masks need to be considered to reduce environmental pollution.

6.3 Identity Security Monitoring

The security threats in daily life are complex. With the rapid development of smart wearable devices, these devices have also become targets of attackers, thus endangering user safety. [202] Consequently, security updates are essential to counter the emergence of new attacks.[203] In the domain of security monitoring, applications such as confidential keypads, path monitoring, and access control systems enhance the security of homes and businesses by enabling real-time monitoring of security conditions through intelligent technologies.[204]

Keyboards, which play a crucial role in connecting the physical and digital worlds in work, study, finance, and entertainment, are often overlooked in terms of security.[205] To eliminate password-based authentication, vulnerable to common attacks like dictionary attacks at present, security strategy combining EMG with TENG technology is proposed. TENG technology enriches the dimensions of data collection and enhances the accuracy of identity verification.[206] Contact and separation between aluminum foil and PTFE film in the EMG sensor also generate triboelectricity. An authentication system based on the dynamics sensors of keystrokes and biometric protection can be easily installed on commercial keyboards (**Figure 17**a). In addition to improving traditional keyboard, creating fully flexible fabric keyboards is also of great significance. The all-fabric-based flexible triboelectric nanogenerator (F-TENG) can respond to tiny pressure changes for real-time biometric authentication (Figure 17b).[207] Leveraging these technologies, a self-powered wearable keyboard (SPWK) was fabricated by integrating a large-area F-TENG sensor array. This SPWK tracks and records electrophysiological signals and identifies individual typing traits via Haar wavelets to distinguish administrators from intruders (Figure 17c).

Industrialization processes and human operational activities in high-risk zones,[208] exemplified by laboratories and chemical plants, pose a significant threat, elevating the probabilities of severe burn incidents and casualties.[209] Therefore, a smart anti-chemical protective suit integrating bio-motor energy harvesting and a self-powered safety monitoring system has been developed (Figure 17d).[210] The core element is all-fiber single electrode TENG yarn (SETY), which has good resistance to acids and alkalis. The suit incorporates highly sensitive chemical sensors to detect chemical leaks. Via integrated physiological monitoring modules, it continuously tracks vital signs. In emergency scenarios where preset thresholds of hazardous chemical concentrations are surpassed, an automated alarm system is instantaneously activated. By monitoring vital signs and movement status, the suit provides real-time alarms to ensure the safety of the wearer. Fire also poses a serious threat to personal safety.[211,212] A 3D honeycomb-structured woven fabric triboelectric nanogenerator (F-TENG) was also woven (Figure 17e) with continuous full-fiber flame-retardant

View Article Online
DOI: 10.1039/D5EE00144G

single-electrode triboelectric yarn (FRTY) as warp and weft yarns.[213] The prepared FRTY can be used to build smart carpets for escape and rescue systems. The F-TENG system has four major functions: flame retardant, real-time route guidance, precise rescue localization and noise reduction.

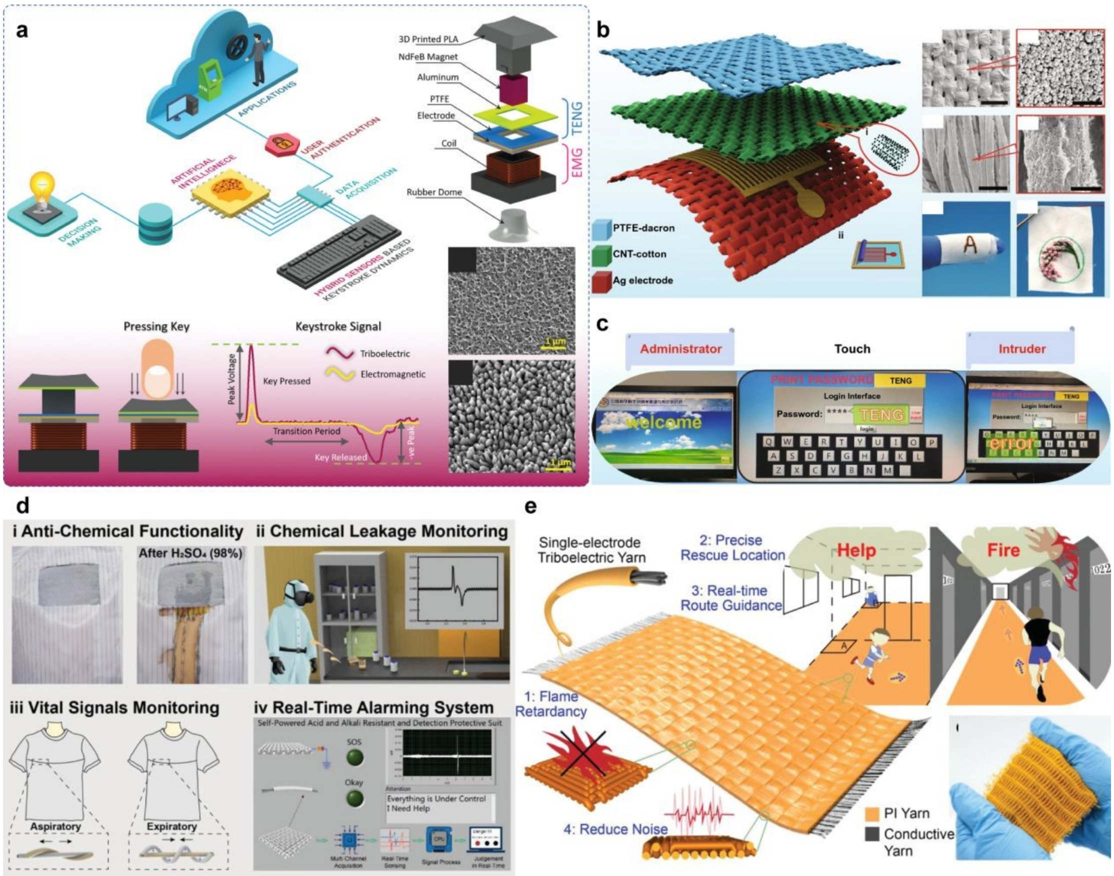

Figure 17. MECFs for security keypad and access control system in security monitoring. a) The working principle of hybrid sensors-driven biometric authentication system. Reproduced with permission.[206] Copyright 2021, Wiley-VCH. b) Schematic diagram of the structural design of the all-fabric-based flexible triboelectric. c) SPWK with self-security features to identify administrators and intruders. b–c) Reproduced with permission.[207] Copyright 2021, Springer Nature. d) Schematic of anti-chemical protective suit, which has four functions of anti-chemical property, chemical leakage monitoring, vital signal monitoring, and real-time alarm system. Reproduced with permission.[210] Copyright 2021, Wiley-VCH. e) Schematic of the intelligent carpet with 3D honeycomb-structured woven F-TENG and Photograph of the prepared F-TENG. Reproduced with permission.[213] Copyright 2020, Wiley-VCH.

Security monitoring technology is undergoing rapid development and continuous innovation. From secure keypads based on keystroke dynamics and biometric protection, to smart floor path monitoring and self-powered access control systems, these technologies greatly improved the security of smart homes. Nevertheless,

View Article Online
DOI: 10.1039/D5EE00144G

several key challenges remain to be tackled in the future. These primarily involve enhancing the resilience of the system against new types of attacks and promoting the standardization of security updates and maintenance procedures. With the continuous advancement of AI and big data technology, combined with more advanced data analysis and predictive models, the performance and user experience of security systems will be further optimized.[214]

7. Summary and Outlook

7.1 Summary

MECFs achieve seamless integration of TENG technology with intelligent textiles, thereby enabling dual-functional operation in both energy harvesting and multimodal information perception. This integration presents an optimized solution for addressing the critical challenges of sustainable power supply and enhanced sensing capabilities in intelligent systems. Technological advancement manifests primarily through two innovative dimensions: (1) the textile substrate demonstrates inherent flexibility, physiological compatibility, and scalable manufacturability, effectively reconciling the inherent conflict between wearability and functional extensibility in conventional devices; (2) the system's fundamental breakthrough originates from TENG's distinctive energy conversion paradigm, enabling simultaneous harvesting of biomechanical energy from human motion and translation of mechanical stimuli into quantifiable electrical signals. This implementation derives from rigorous analysis of human biomechanics as a dual-aspect system, acting simultaneously as a continuous mechanical energy source and an energy consumption terminal. Through the integration of TENG into textiles, the developed system not only successfully achieves the efficient conversion of human mechanical energy into electrical energy but also constructs a self-powered sensing network through structural innovation, fundamentally solving the longstanding challenge of separating sensing systems from external power dependence on traditional wearable devices. Hence, subsequent to clarifying this practical requirement, we initially delved into the fundamental principles underlying the energy harvesting and self-powered sensing of TENGs. We also reviewed the manufacturing techniques and morphological characteristics of textiles functioning as large-area affiliated carriers and application platforms for TENGs. Emphasis was placed on the novel type of flexible wearable self-powered textile, namely MECF. A comprehensive investigation and detailed discussion were then conducted regarding the current innovative applications of MECF. For each category, including (1) personalized smart healthcare, (2) wearable electronic products and AI, and (3) environmental safety and personal protection, recent research efforts were outlined, and corresponding discussions were provided.

7.2 Future Development

MECF represents an exemplary combination of TENG technology and textiles. Therefore, in the analysis of the problems and future development directions of MECF, it is necessary to consider both the common problems of TENG technology and the specific problems in emerging fields of MECF.

View Article Online
DOI: 10.1039/D5EE00144G

The common problems of TENG:

(1) In energy acquisition, the electrical output of TENG is characterized by a high voltage alternating current (AC) pulse, which is inconsistent with the constant direct current (DC) voltage required by wearable electronic devices. This characteristic also results in the output of TENG being efficient only under high-resistance conditions, which significantly differs from the impedance of electronic products. The power output of TENG is still below the actual requirements of most wearable electronic products. Currently, there are several methods to enhance the energy conversion efficiency of MECF, such as increasing the effective contact area, improving the softness, establishing a nanostructured contact interface, and using hybrid energy harvesters.

(2) In flexible smart sensing, TENG still lacks linearity and anti-interference capabilities, which is a significant gap from the ideal sensing signal. And the triboelectric charge density is greatly affected by environmental temperature and humidity. In addition, during practical use, after complex, repetitive, and intense external mechanical loads or chemical treatments, the electrical output of MECF may be drastically reduced. In frequent use, contaminants will inevitably be absorbed on the surface of TENG, which will reduce the electrical output due to weakened charge transfer. It should be noted that these environmental factors are not fatal to TENG, as the electrical output performance can be restored when the environmental conditions are eliminated.

The common problems of textiles:

(1) Comfort, durability, and safety. Textile-based TENGs for wearable purposes must meet various requirements including flexibility, stretchability, breathability, washability, cutability, biocompatibility, and aesthetics. Unfortunately, most of the current fibrous conductive materials are either too hard or too soft. For example, most flexible polymers are prone to fracture under intense mechanical loads, while metal wires/foils are too hard for textile-based TENGs. In addition to the above requirements, tactile comforts such as prickling sensation, fabric weight, static electricity, and cold stimuli are also important for abrasion resistance. The thorny problem of textile-based TENGs based on customized textiles is circuit connection. Machine washability is particularly important for textile-based TENGs as it concerns whether they can be used multiple times.

(2) Industrial Manufacturing. The large-scale industrial production of textile-based TENG is one of the fundamental prerequisites for its wide commercial application. However, disappointingly, most of the MECFs reported above are manufactured by hand. From the perspective of materials and structural design, it is rather difficult to coat the functional materials on their surfaces or find a textile structure that can be fabricated quickly and worn well. Most functional fibers are incompatible with the mature textile manufacturing processes.

The common problems represent the trade-off between the performance of TENGs and the comfort as well as the robustness of textiles. The focus of future research is on exploring how to balance the enhancement of conductivity and functionality with the improvement of comfort and production scalability. Upon comprehensive consideration of the working mechanism of TENG and the design principles of textiles, in light of the practical requirements within emerging application domains, MECF still possesses extensive prospects for development (**Figure 18**).

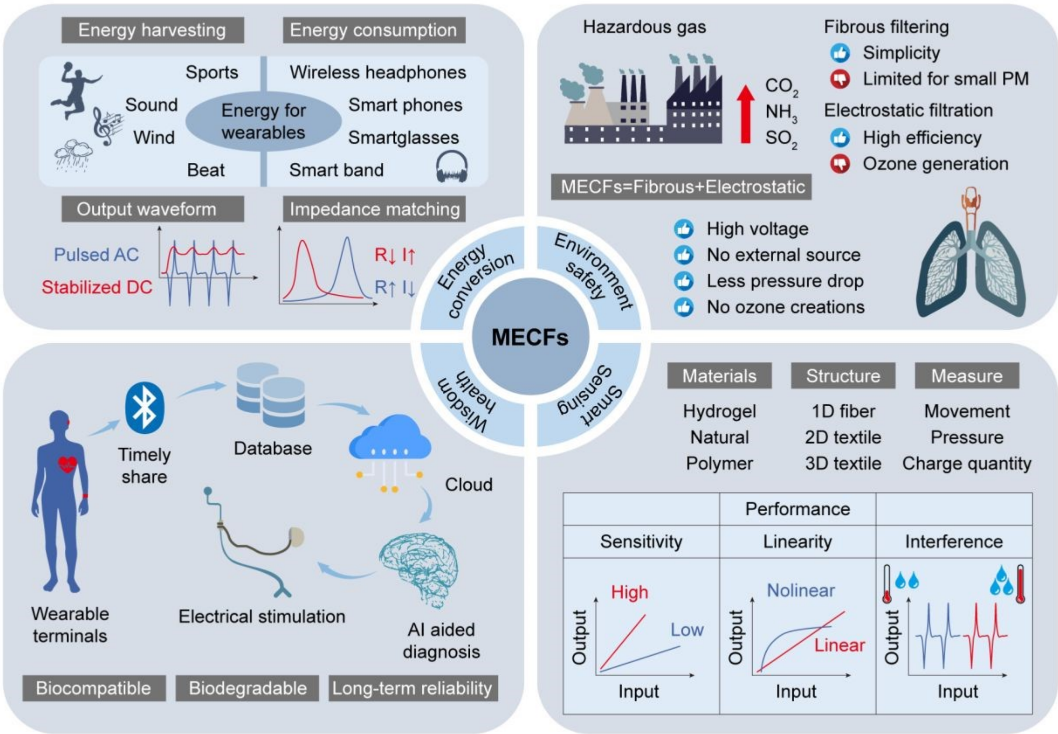

Figure 18. Conclusions and perspectives regarding MECF for advanced self-powered sensing applications. It summarizes the achievements made from energy acquisition to intelligent application in a complete closed loop and highlights the pressing issues that need to be addressed in the application of various fields.

Specifically, the development trend of MECF in personalized healthcare:

(1) Multi-modal high precision sensing. In addition to monitoring conventional cardiovascular and respiratory parameters, MECF's applications could be broadened to include real-time tracking of neural electrical activities (neuron firing frequency, nerve conduction velocity, etc.) and muscle tension. Furthermore, integrating MECF with other imaging modalities, like ultrasound or optical imaging, could enable the visualization of human tissue and organ functions, aiding in the diagnosis of tumors, cardiovascular conditions, neurological disorders, and providing a more intuitive and precise foundation for early disease detection and treatment.

(2) Assisting in disease treatment through precise adjustment. Leveraging advancements in medical tissue engineering and regenerative medicine, MECF could employ its electrical signaling to modulate the characteristics of bioelectroactive materials, thereby promoting cell proliferation, differentiation, and extracellular matrix secretion, and guiding the direction and process of

View Article Online
DOI: 10.1039/D5EE00144G

tissue regeneration. Additionally, a TENG-based smart drug delivery system could be developed to precisely control the timing, dosage, and rate of drug release in response to therapeutic needs and physiological feedback. For instance, in cancer therapy, TENG-generated electrical stimulation could enhance tumor cells' sensitivity to chemotherapy while improving drug penetration and distribution within the tumor tissue, thus enhancing efficacy and reducing side effects.

(3) Telemedicine and health management: towards professionalism. To advance telemedicine and professional health management, MECF could aggregate and analyze multi-source data from various physiological parameters, monitoring sites, and time points. By developing intelligent diagnostic algorithms grounded in deep learning, models can be trained to discern patterns in normal physiological states and different disease states, providing prediction for health risk assessments or personalized medical recommendations, thereby enabling automated disease diagnosis and risk evaluation. Continual accumulation of clinical data and algorithm refinement would further enhance diagnostic accuracy and efficiency, supporting the advancement of personalized medicine.

The development trend of MECF in IoT and HMI:

(1) Innovative sensing interaction modes. For multimodal interaction, integrating various TENG sensors enables the detection of multiple input methods, including pressure, touch, and bending, thereby enriching the user interaction experience. For non-contact interaction, non-contact TENG sensors are developed to reduce direct contact, enhance device stability and longevity, and are suitable for applications like automatic position detection. Furthermore, for intelligent energy management, AI algorithms assist in optimizing energy distribution and management by analyzing real-time power consumption and energy harvesting data from the device.

(2) Emerging application scenarios. In motion capture, MECFs enable the precise tracking of human body movements, leading to more natural and accurate mapping of virtual character actions. In industrial manufacturing, MECFs are employed to monitor equipment status, thus enhancing production efficiency and safety. In gaming and entertainment, integrating MECFs into game controllers or motion-sensing devices can bring a more realistic gaming experience. In intelligent transportation, applying MECFs to the HMI system of vehicles supports real-time monitoring of the driver's condition and vehicle control.

(3) Immersive virtual teaching and training environments: In education, MECF-based touchable learning devices can be developed to enhance student engagement and improve learning outcomes. In vocational training fields such as aerospace, medical surgery, and mechanical equipment operation, VR and HMI technologies are utilized to construct simulated training platforms. Trainees can perform hands-on training in these virtual environments, where the system monitors their operational movements, applied forces, reaction times, and other parameters in real time with MECFs. This setup provides immediate

feedback and guidance, allowing trainees to refine their skills in a safe environment and minimize errors and risks during actual operations.

The development trend of MECF in environmental safety and personal protection:

(1) The responsiveness of TENG to non-target gases can be reduced and the selectivity for the detection of specific hazardous gases can be enhanced through methods such as functional group modification and material screening. For example, in industrial environments where multiple gases coexist, MECF-based sensors can be designed to specifically detect one or more critical hazardous gases. Meanwhile, multi-parameter joint detection can be achieved by integrating MECFs with electrochemical and optical sensors, among others, to create a comprehensive gas monitoring system that evaluates ambient air quality and pollution sources in greater detail. Nanofiber materials with high specific surface area and special adsorption properties can be developed, and composite filter materials with multi-level structures can be prepared to strengthen the capturing ability of particulate matter.

(2) MECF will be committed to combining with other monitoring methods to achieve real-time monitoring of indoor air quality (e.g., PM2.5, formaldehyde, and volatile organic compounds), water quality (e.g., pH scale, dissolved oxygen, and heavy metal ion concentrations), and electrical safety (e.g., leakage current and overload). By linking with the smart home system, MECF can automatically trigger appropriate responses to ensure the safety and health of the household environment. In addition, MECF can be introduced as contactless identification office equipment. Contactless identification technologies can be used in scenarios such as office access control, computer login, and file encryption.

(3) In emergency rescue scenarios, MECFs can be utilized for real-time positioning and monitoring of both rescue workers and trapped individuals. These wearable devices can transmit vital signs (such as heart rate and body temperature) and surrounding environmental information (such as the concentration of hazardous gases and temperature) in real time, while also providing protection against toxic substances. For trapped individuals, the MECF sensor network deployed in the rescue area can rapidly pinpoint their locations and assess their physical condition, providing critical support for rescue efforts. Meanwhile, devices such as MECF smart carpets can provide real-time route guidance on the rescue site, helping rescue workers and trapped people to evacuate the dangerous area quickly and safely.

Research on these issues will open a new stage for the development of MECF. Grounded in the fundamental principles of self-sufficiency and serving life, leveraging the wearing convenience and design flexibility of fabric-based materials, our efforts will focus on continuously enhancing energy output and sensitivity. This will enable us to deliver superior services in supporting people's physical and mental well-being, facilitating intelligent interactions, and ensuring security and defense.

Author Contributions

Conceptualization, K.D.; Funding acquisition, J.Z., X.P., K.D.; Investigation, J.Z, X.F., H.X., Y.L. and Z.L.; Supervision, G.T., Z.W., K.D.; Writing - original draft, J.Z, X.F., H.X., Y.L. and Z.L.; Writing - review & editing, J.Z., Z.W., K.D.

Conflicts of Interest

There are no conflicts to declare.

Data Availability

No primary research results, software or code, have been included and no new data was generated or analyzed as part of this review.

Acknowledgements

The authors are grateful for the support received from the National Natural Science Foundation of China (grant No. 22109012), the Natural Science Foundation of the Beijing Municipality (grant No. L222037 and 2212052), China Postdoctoral Science Foundation (Grant No. 2024M753175 and 2024M751716), the Postdoctoral Fellowship Program of CPSF (Grant No. GZC20232612 and GZB20230328), the Fundamental Research Funds for the Central Universities (grant No. E1E46805), and the ShuiMu Tsinghua Scholar Program.

References

1. Q. Zheng, Q. Tang, Z. L. Wang and Z. Li, *Nat Rev Cardiol*, 2021, **18**, 7-21.
2. T. Cheng, J. Shao and Z. L. Wang, *Nature Reviews Methods Primers*, 2023, **3**, 39.
3. H. Xiang, L. Peng, Q. Yang, Z. L. Wang and X. Cao, *Sci Adv*, 2024, **10**, eads2291.
4. C. Xu, Y. Zi, A. C. Wang, H. Zou, Y. Dai, X. He, P. Wang, Y. C. Wang, P. Feng, D. Li and Z. L. Wang, *Adv. Mater.*, 2018, **30**, e1706790.
5. J. Luo, W. Gao and Z. L. Wang, *Adv. Mater.*, 2021, **33**, e2004178.
6. L. Zhou, D. Liu, L. Ren, H. Xue, B. Li, S. Niu, Q. Liu, Z. Han and L. Ren, *ACS Nano*, 2022, **16**, 7721-7731.
7. B. Dong, Q. Shi, T. He, S. Zhu, Z. Zhang, Z. Sun, Y. Ma, D. L. Kwong and C. Lee, *Adv Sci (Weinh)*, 2020, **7**, 1903636.
8. P. Pandey, D.-H. Jung, G.-J. Choi, M.-K. Seo, S. Lee, J. M. Kim, I.-K. Park and J. I. Sohn, *Nano Energy*, 2023, **107**, 108134.
9. C. Zhao, T. Du, B. Ge, Z. Xi, Z. Qian, Y. Wang, J. Wang, F. Dong, D. Shen, Z. Zhan and M. Xu, *Small*, 2024, **20**, e2307680.
10. K. Dong, X. Peng, R. Cheng, C. Ning, Y. Jiang, Y. Zhang and Z. L. Wang, *Adv. Mater.*, 2022, **34**, e2109355.
11. J. Z. Zhao, Y. Yao, W. T. Lei, L. Zhao, A. D. Liu, M. D. Ye, J. Y. Wu, S. H. Guo and W. X. Guo, *Nano Energy*, 2023, **113**, 108534.
12. Y. Zi, H. Guo, Z. Wen, M. H. Yeh, C. Hu and Z. L. Wang, *ACS Nano*, 2016, **10**, 4797-4805.
13. Z. L. Wang, *Advances in Physics-X*, 2024, **9**, 2354767.

View Article Online
DOI: 10.1039/D5EE00144G

14. Z. L. Wang, *Mater. Today*, 2022, **52**, 348-363.
15. Z. L. Wang, *Nano Energy*, 2020, **68**, 104272.
16. Z. L. Wang, *Journal of Physics Communications*, 2024, **8**, 115004.
17. L. H. Jiang, X. L. Liu, J. L. Lv, G. J. Li, P. Y. Yang, Y. M. Ma, H. Y. Zou and Z. L. Wang, *Energy & Environmental Science*, 2024, **17**, 3700-3738.
18. Z. L. Wang and A. C. Wang, *Mater. Today*, 2019, **30**, 34-51.
19. S. Lin, L. Xu, A. Chi Wang and Z. L. Wang, *Nat Commun*, 2020, **11**, 399.
20. Z. L. Wang, *Advanced Energy Materials*, 2020, **10**, 2000137.
21. J. Wang, S. Y. Xu, G. Li, H. Y. Wu, K. X. Li, A. Chen, Q. H. Zhao, S. K. Fu, C. C. Shan, Y. Xi and C. G. Hu, *Energy & Environmental Science*, 2024, **17**, 7382-7393.
22. X. L. Tao, X. Y. Chen and Z. L. Wang, *Energy & Environmental Science*, 2023, **16**, 3654-3678.
23. Q. H. Zhao, H. Y. Wu, J. Wang, S. Y. Xu, W. C. He, C. C. Shan, S. K. Fu, G. Li, K. X. Li and C. G. Hu, *Advanced Energy Materials*, 2023, **13**, 2302099.
24. J. Wang, H. Y. Wu, S. K. Fu, G. Li, C. C. Shan, W. C. He and C. G. Hu, *Nano Energy*, 2022, **104**, 107916.
25. Y. B. Nan, X. T. Wang, H. Xu, Y. Wu, H. Zhou, Y. A. Sun, T. Yu and Y. L. Huang, *Nano Energy*, 2023, **110**, 108345.
26. N. Y. Cui, J. M. Liu, Y. M. Lei, L. Gu, Q. Xu, S. H. Liu and Y. Qin, *Acs Applied Energy Materials*, 2018, **1**, 2891-2897.
27. X. Xie, Y. Fang, C. Lu, Y. Tao, L. Yin, Y. Zhang, Z. Wang, S. Wang, J. Zhao, X. Tu, X. Sun, E. G. Lim, C. Zhao, Y. Liu and Z. Wen, *Chem. Eng. J.*, 2023, **452**, 139469.
28. X. Lv, Y. Liu, J. Yu, Z. Li and B. Ding, *Advanced Fiber Materials*, 2022, **5**, 401-428.
29. C. Y. Chen, L. J. Chen, Z. Y. Wu, H. Y. Guo, W. D. Yu, Z. Q. Du and Z. L. Wang, *Mater. Today*, 2020, **32**, 84-93.
30. C. Ning, R. Cheng, Y. Jiang, F. Sheng, J. Yi, S. Shen, Y. Zhang, X. Peng, K. Dong and Z. L. Wang, *ACS Nano*, 2022, **16**, 2811-2821.
31. R. W. Cheng, C. Ning, P. F. Chen, F. F. Sheng, C. H. Wei, Y. H. Zhang, X. Peng, K. Dong and Z. L. Wang, *Advanced Energy Materials*, 2022, **12**, 2201532.
32. Y. P. Zhang, C. Y. Li, C. H. Wei, R. W. Cheng, T. M. Lv, J. P. Wang, C. Zhao, Z. Y. Wang, F. M. Li, X. Peng, M. Y. Xu and K. Dong, *Infomat*, 2024, **6**, e12534.
33. X. Pu, W. X. Song, M. M. Liu, C. W. Sun, C. H. Du, C. Y. Jiang, X. Huang, D. C. Zou, W. G. Hu and Z. L. Wang, *Advanced Energy Materials*, 2016, **6**, 1601048.
34. I. Ali, M. R. Islam, J. Yin, S. J. Eichhorn, J. Chen, N. Karim and S. Afroj, *ACS Nano*, 2024, **18**, 3871-3915.
35. C. Ning, G. Zheng and K. Dong, *Advanced Sensor Research*, 2023, **2**, 2200044.
36. A. Fakharuddin, H. Z. Li, F. Di Giacomo, T. Y. Zhang, N. Gasparini, A. Y.

DOI: 10.1039/D5EE00144G

Elezzabi, A. Mohanty, A. Ramadoss, J. Ling, A. Soultati, M. Tountas, L. Schmidt-Mende, P. Argitis, R. Jose, M. K. Nazeeruddin, A. B. Yusoff and M. Vasilopoulou, *Advanced Energy Materials*, 2021, **11**, 2101443.
37. J. Z. Zhao, D. W. Chen, L. Zhao, Y. T. Shi, S. H. Guo, Z. G. Zhu, J. R. Liu, W. J. Li, W. T. Lei, H. X. Chen, Y. Chen, D. Zhou, R. H. Wu and W. X. Guo, *Cell Reports Physical Science*, 2022, **3**, 101168.
38. J. L. Li, J. Y. Cai, J. Y. Yu, Z. L. Li and B. Ding, *Adv. Funct. Mater.*, 2023, **33**, 2303249.
39. K. Dong, X. Peng and Z. L. Wang, *Adv. Mater.*, 2020, **32**, e1902549.
40. Y. Wang, L. Chu, S. Meng, M. Yang, Y. Yu, X. Deng, C. Qi, T. Kong and Z. Liu, *Adv Sci (Weinh)*, 2024, **11**, e2401436.
41. S. Lin, W. Yang, X. Zhu, Y. Lan, K. Li, Q. Zhang, Y. Li, C. Hou and H. Wang, *Nat Commun*, 2024, **15**, 2374.
42. T. T. Jing, B. G. Xu and Y. J. Yang, *Nano Energy*, 2021, **84**, 105867.
43. Y. P. Wu, X. Y. Dai, Z. H. Sun, S. X. Zhu, L. Xiong, Q. H. Liang, M. C. Wong, L. B. A. Huang, Q. Qin and J. H. Hao, *Nano Energy*, 2022, **98**, 107240.
44. W. Yang, W. Gong, W. Gu, Z. Liu, C. Hou, Y. Li, Q. Zhang and H. Wang, *Adv. Mater.*, 2021, **33**, e2104681.
45. Z. Li, B. Xu, J. Han, J. Huang and H. Fu, *Adv. Funct. Mater.*, 2021, **32**, 2106731.
46. S. S. Dong, F. Xu, Y. L. Sheng, Z. H. Guo, X. Pu and Y. P. Liu, *Nano Energy*, 2020, **78**, 105327.
47. Y. Jiang, K. Dong, X. Li, J. An, D. Wu, X. Peng, J. Yi, C. Ning, R. Cheng, P. Yu and Z. L. Wang, *Adv. Funct. Mater.*, 2020, **31**, 2005584.
48. R. H. Wu, S. Liu, Z. F. Lin, S. H. Zhu, L. Y. Ma and Z. L. Wang, *Advanced Energy Materials*, 2022, **12**, 2201288.
49. Y. Xiong, L. Luo, J. H. Yang, J. Han, Y. Liu, H. S. Jiao, S. S. Wu, L. Q. Cheng, Z. Y. Feng, J. Sun, Z. L. Wang and Q. J. Sun, *Nano Energy*, 2023, **107**, 108137.
50. K. Dong, X. Peng, J. An, A. C. Wang, J. Luo, B. Sun, J. Wang and Z. L. Wang, *Nat Commun*, 2020, **11**, 2868.
51. J. Xiong, P. Cui, X. Chen, J. Wang, K. Parida, M. F. Lin and P. S. Lee, *Nat Commun*, 2018, **9**, 4280.
52. W. Paosangthong, M. Wagih, R. Torah and S. Beeby, *Nano Energy*, 2022, **92**, 106739.
53. Z. Feng, S. Yang, S. X. Jia, Y. J. Zhang, S. Jiang, L. Yu, R. Li, G. W. Song, A. B. Wang, T. Martin, L. Zuo and X. T. Jia, *Nano Energy*, 2020, **74**, 104805.
54. Z. Zhao, L. Zhou, S. Li, D. Liu, Y. Li, Y. Gao, Y. Liu, Y. Dai, J. Wang and Z. L. Wang, *Nat Commun*, 2021, **12**, 4686.
55. Z. Jin, L. Wang, K. Zheng, Q. Gao, W. Feng, S. Hu, M. Yue and X. Shan, *J. Colloid Interface Sci.*, 2024, **669**, 275-282.
56. H. Duo, H. Wang, S. Shima, E. Takamura and H. Sakamoto, *Nano Energy*, 2024, **131**, 110297.
57. G. Khandelwal, G. Min, X. Karagiorgis and R. Dahiya, *Nano Energy*, 2023,

View Article Online
DOI: 10.1039/D5EE00144G

110, 108325.
58. Y. Hao, Y. Zhang, A. Mensah, S. Liao, P. Lv and Q. Wei, *Nano Energy*, 2023, **109**, 108291.
59. W. Li, L. Lu, F. Yan, G. Palasantzas, K. Loos and Y. Pei, *Nano Energy*, 2023, **114**, 108629.
60. Y. Wu, X. Dai, Z. Sun, S. Zhu, L. Xiong, Q. Liang, M.-C. Wong, L.-B. Huang, Q. Qin and J. Hao, *Nano Energy*, 2022, **98**, 107240.
61. M. S. B. Sadeque, M. Rahman, M. M. Hasan and M. Ordu, *Advanced Electronic Materials*, 2024, **10**, 2300643.
62. Y. He, A. C. Y. Goay, A. C. Y. Yuen, D. Mishra, Y. Zhou, T. Lu, D. Wang, Y. Liu, C. Boyer, C. H. Wang and J. Zhang, *Adv Sci (Weinh)*, 2024, **11**, e2305829.
63. Y. Li, J. Xiong, J. Lv, J. Chen, D. Gao, X. Zhang and P. S. Lee, *Nano Energy*, 2020, **78**, 105358.
64. Y. Yang, Y. Yang, J. Huang, S. Li, Z. Meng, W. Cai and Y. Lai, *Advanced Fiber Materials*, 2023, **5**, 1505-1518.
65. J. Fan, M. Yuan, L. Wang, Q. Xia, H. Zheng and A. Zhou, *Nano Energy*, 2023, **105**, 107973.
66. W. Paosangthong, R. Torah and S. Beeby, *Nano Energy*, 2019, **55**, 401-423.
67. L. Lan, J. Xiong, D. Gao, Y. Li, J. Chen, J. Lv, J. Ping, Y. Ying and P. S. Lee, *ACS Nano*, 2021, **15**, 5307-5315.
68. X. Karagiorgis, D. Shakthivel, G. Khandelwal, R. Ginesi, P. J. Skabara and R. Dahiya, *ACS Appl Mater Interfaces*, 2024, **16**, 19551-19562.
69. L. L. Shang, Z. P. Wu, X. Y. Li, A. Xu, Y. Miao, W. L. Xu, W. Y. Tang, C. Y. Fu, B. Su, K. Dong and Z. G. Xia, *Nano Energy*, 2023, **118**, 108955.
70. S. S. H. Abir, M. U. K. Sadaf, S. K. Saha, A. Touhami, K. Lozano and M. J. Uddin, *ACS Appl Mater Interfaces*, 2021, **13**, 60401-60412.
71. Y. Li, S. Xiao, X. X. Zhang, P. Jia, S. S. Tian, C. Pan, F. P. Zeng, D. C. Chen, Y. Y. Chen, J. Tang and J. Q. Xiong, *Nano Energy*, 2022, **98**, 107347.
72. J. B. Yu, X. J. Hou, J. He, M. Cui, C. Wang, W. P. Geng, J. L. Mu, B. Han and X. J. Chou, *Nano Energy*, 2020, **69**, 104437.
73. Y. Zhang, D. S. Zhang, Y. Y. Chen, H. Lin, X. R. Zhou, Y. F. Zhang and J. Q. Xiong, *Advanced Materials Technologies*, 2023, **8**, 2202030.
74. B. Yu, J. Long, T. Huang, Z. Xiang, M. Liu, X. Zhang, J. Zhu and H. Yu, *ACS Omega*, 2023, **8**, 31427-31435.
75. M. M. Hasan, M. S. B. Sadeque, I. Albasar, H. Pecenek, F. K. Dokan, M. S. Onses and M. Ordu, *Small*, 2023, **19**, e2206107.
76. Y. X. Chen, Z. R. Deng, R. Ouyang, R. H. Zheng, Z. Q. Jiang, H. Bai and H. Xue, *Nano Energy*, 2021, **84**, 105866.
77. S. Lee, J. Kim, I. Yun, G. Y. Bae, D. Kim, S. Park, I. M. Yi, W. Moon, Y. Chung and K. Cho, *Nat Commun*, 2019, **10**, 2468.
78. T. S. Dinh Le, J. An, Y. Huang, Q. Vo, J. Boonruangkan, T. Tran, S. W. Kim, G. Sun and Y. J. Kim, *ACS Nano*, 2019, **13**, 13293-13303.
79. F. Xu, J. Yang, R. Z. Dong, H. X. Jiang, C. H. Wang, W. L. Liu, Z. X. Jiang,

X. Q. Zhang and G. D. Zhu, *Advanced Fiber Materials*, 2021, **3**, 368-380.
80. W. Yang, W. Gong, C. Hou, Y. Su, Y. Guo, W. Zhang, Y. Li, Q. Zhang and H. Wang, *Nat Commun*, 2019, **10**, 5541.
81. T. Sun, B. Zhou, Q. Zheng, L. Wang, W. Jiang and G. J. Snyder, *Nat Commun*, 2020, **11**, 572.
82. J. Zou, F. Ling, X. Shi, K. Xu, H. Wu, P. Chen, B. Zhang, D. Ta and H. Peng, *Small*, 2021, **17**, e2102052.
83. Y. H. Jung, S. K. Hong, H. S. Wang, J. H. Han, T. X. Pham, H. Park, J. Kim, S. Kang, C. D. Yoo and K. J. Lee, *Adv. Mater.*, 2020, **32**, e1904020.
84. A. Libanori, G. R. Chen, X. Zhao, Y. H. Zhou and J. Chen, *Nature Electronics*, 2022, **5**, 142-156.
85. K. Y. Meng, S. L. Zhao, Y. H. Zhou, Y. F. Wu, S. L. Zhang, Q. He, X. Wang, Z. H. Zhou, W. J. Fan, X. L. Tan, J. Yang and J. Chen, *Matter*, 2020, **2**, 896-907.
86. G. Chen, X. Zhao, S. Andalib, J. Xu, Y. Zhou, T. Tat, K. Lin and J. Chen, *Matter*, 2021, **4**, 3725-3740.
87. F. Q. Chen, Y. H. Wu, Z. Y. Ding, X. Xia, S. H. Li, H. W. Zheng, C. L. Diao, G. T. Yue and Y. L. Zi, *Nano Energy*, 2019, **56**, 241-251.
88. L. Q. Liu, X. Y. Yang, L. L. Zhao, W. K. Xu, J. W. Wang, Q. M. Yang and Q. W. Tang, *Nano Energy*, 2020, **73**, 104797.
89. B. K. Deka, A. Hazarika, M. J. Kwak, D. C. Kim, A. P. Jaiswal, H. G. Lee, J. Seo, C. Jeong, J. H. Jang, Y. B. Park and H. W. Park, *Energy Storage Materials*, 2021, **43**, 402-410.
90. P. Y. Feng, Z. Xia, B. Sun, X. Jing, H. Li, X. Tao, H. Y. Mi and Y. Liu, *ACS Appl Mater Interfaces*, 2021, **13**, 16916-16927.
91. C. Li, Z. Xu, S. Xu, T. Wang, S. Zhou, Z. Sun, Z. L. Wang and W. Tang, *Nano Res*, 2023, DOI: 10.1007/s12274-023-5420-1, 1-9.
92. T. Huang, J. Zhang, B. Yu, H. Yu, H. R. Long, H. Z. Wang, Q. H. Zhang and M. F. Zhu, *Nano Energy*, 2019, **58**, 375-383.
93. Y. B. Wang, M. M. Zhu, X. D. Wei, J. Y. Yu, Z. L. Li and B. Ding, *Chem. Eng. J.*, 2021, **425**, 130599.
94. H. Xu, J. Tao, Y. Liu, Y. Mo, R. Bao and C. Pan, *Small*, 2022, **18**, e2202477.
95. Y. Q. Lei, J. H. Yang, Y. Xiong, S. S. Wu, W. D. Guo, G. S. Liu, Q. J. Sun and Z. L. Wang, *Chem. Eng. J.*, 2023, **462**, 142170.
96. T. Tat, A. Libanori, C. Au, A. Yau and J. Chen, *Biosens. Bioelectron.*, 2021, **171**, 112714.
97. W. J. Li, Y. T. Pei, C. Zhang and A. G. P. Kottapalli, *Nano Energy*, 2021, **84**, 105865.
98. T. Zhao, Y. Fu, C. Sun, X. Zhao, C. Jiao, A. Du, Q. Wang, Y. Mao and B. Liu, *Biosens. Bioelectron.*, 2022, **205**, 114115.
99. R. L. Bulathsinghala, W. Ding and R. D. I. G. Dharmasena, *Nano Energy*, 2023, **116**, 108792.
100. Y. Yang, Y. Yang, J. Huang, S. Li, Z. Meng, W. Cai and Y. Lai, *Adv Fiber Mater*, 2023, **5**, 1-14.

101. F. Sheng, C. Zhao, B. Zhang, Y. Tan and K. Dong, *Soft Science*, 2024, **4**, 2.
102. L. Y. Ma, W. W. Chen, R. L. Gao, L. S. Liu, M. L. Zhu, Y. J. Wang, Z. S. Wu, H. J. Li, D. F. Gu, Y. J. Yang, Z. Zheng and S. S. Hu, *J Geriatr Cardiol*, 2020, **17**, 1-8.
103. F. Sana, E. M. Isselbacher, J. P. Singh, E. K. Heist, B. Pathik and A. A. Armoundas, *J Am Coll Cardiol*, 2020, **75**, 1582-1592.
104. X. Ding, B. P. Yan, Y. T. Zhang, J. Liu, N. Zhao and H. K. Tsang, *Sci Rep*, 2017, **7**, 11554.
105. Y. Ma, J. Choi, A. Hourlier-Fargette, Y. Xue, H. U. Chung, J. Y. Lee, X. Wang, Z. Xie, D. Kang, H. Wang, S. Han, S. K. Kang, Y. Kang, X. Yu, M. J. Slepian, M. S. Raj, J. B. Model, X. Feng, R. Ghaffari, J. A. Rogers and Y. Huang, *Proc Natl Acad Sci U S A*, 2018, **115**, 11144-11149.
106. M. O. G. Nayeem, S. Lee, H. Jin, N. Matsuhisa, H. Jinno, A. Miyamoto, T. Yokota and T. Someya, *Proc Natl Acad Sci U S A*, 2020, **117**, 7063-7070.
107. S. C. Fang, Y. L. Wu and P. S. Tsai, *Biol Res Nurs*, 2020, **22**, 45-56.
108. J. Mensah-Kane, A. F. Schmidt, A. D. Hingorani, C. Finan, Y. Chen, S. van Duijvenboden, M. Orini, P. D. Lambiase, A. Tinker, E. Marouli, P. B. Munroe and J. Ramirez, *Front Genet*, 2021, **12**, 569323.
109. S. Li, H. Wang, W. Ma, L. Qiu, K. Xia, Y. Zhang, H. Lu, M. Zhu, X. Liang, X. E. Wu, H. Liang and Y. Zhang, *Sci Adv*, 2023, **9**, eadh0615.
110. C. A. Valencia-Hernandez, J. V. Lindbohm, M. J. Shipley, I. B. Wilkinson, C. M. McEniery, S. Ahmadi-Abhari, A. Singh-Manoux, M. Kivimaki and E. J. Brunner, *Hypertension*, 2022, **79**, 836-843.
111. W. Fan, Q. He, K. Meng, X. Tan, Z. Zhou, G. Zhang, J. Yang and Z. L. Wang, *Sci Adv*, 2020, **6**, eaay2840.
112. F. D. Fuchs and P. K. Whelton, *Hypertension*, 2020, **75**, 285-292.
113. X. Wang, Z. P. Feng, Y. S. Xia, G. Q. Zhang, L. A. Wang, L. Chen, Y. F. Wu, J. Yang and Z. L. Wang, *Nano Energy*, 2022, **102**, 107710.
114. K. Meng, J. Chen, X. Li, Y. Wu, W. Fan, Z. Zhou, Q. He, X. Wang, X. Fan, Y. Zhang, J. Yang and Z. L. Wang, *Adv. Funct. Mater.*, 2018, **29**, 1806388.
115. M. Kebe, R. Gadhafi, B. Mohammad, M. Sanduleanu, H. Saleh and M. Al-Qutayri, *Sensors (Basel)*, 2020, **20**, 1454.
116. C. Massaroni, A. Nicolò, M. Sacchetti and E. Schena, *IEEE Sens. J.*, 2021, **21**, 12821-12839.
117. J. Lama, A. Yau, G. R. Chen, A. Sivakumar, X. Zhao and J. Chen, *Journal of Materials Chemistry A*, 2021, **9**, 19149-19178.
118. Y. Fang, J. Xu, X. Xiao, Y. Zou, X. Zhao, Y. Zhou and J. Chen, *Adv. Mater.*, 2022, **34**, e2200252.
119. S. B. Si, C. C. Sun, J. Qiu, J. Liu and J. Yang, *Applied Materials Today*, 2022, **27**, 101508.
120. X. Peng, K. Dong, C. A. Ning, R. W. Cheng, J. Yi, Y. H. Zhang, F. F. Sheng, Z. Y. Wu and Z. L. Wang, *Adv. Funct. Mater.*, 2021, **31**, 2103559.
121. M. E. Hirschtritt, M. P. Walker and A. D. Krystal, *Sleep Science and Practice*, 2023, **7**, 3.

122. K. C. Simon, L. Nadel and J. D. Payne, *Proc Natl Acad Sci U S A*, 2022, **119**, e2201795119.
123. R. R. Gilley, *Clin EEG Neurosci*, 2023, **54**, 12-20.
124. K. Kuna, K. Szewczyk, A. Gabryelska, P. Bialasiewicz, M. Ditmer, D. Strzelecki and M. Sochal, *Biomedicines*, 2022, **10**, 2159.
125. M. Sejbuk, I. Mironczuk-Chodakowska and A. M. Witkowska, *Nutrients*, 2022, **14**, 1912.
126. G. Zoccoli and R. Amici, *Current Opinion in Physiology*, 2020, **15**, 128-133.
127. N. Baranwal, P. K. Yu and N. S. Siegel, *Prog Cardiovasc Dis*, 2023, **77**, 59-69.
128. Z. Zhou, S. Padgett, Z. Cai, G. Conta, Y. Wu, Q. He, S. Zhang, C. Sun, J. Liu, E. Fan, K. Meng, Z. Lin, C. Uy, J. Yang and J. Chen, *Biosens. Bioelectron.*, 2020, **155**, 112064.
129. N. N. Zhang, Y. Z. Li, S. W. Xiang, W. W. Guo, H. Zhang, C. Y. Tao, S. Yang and X. Fan, *Nano Energy*, 2020, **72**, 104664.
130. H. Kou, H. Wang, R. Cheng, Y. Liao, X. Shi, J. Luo, D. Li and Z. L. Wang, *ACS Appl Mater Interfaces*, 2022, **14**, 23998-24007.
131. O. Yue, X. Wang, M. Hou, M. Zheng, Z. Bai, B. Cui, S. Cha and X. Liu, *Nano Energy*, 2022, **91**, 106682.
132. R. Wu, L. Ma and X. Y. Liu, *Adv Sci (Weinh)*, 2022, **9**, e2103981.
133. H. Kim, B. Rigo, G. Wong, Y. J. Lee and W. H. Yeo, *Nanomicro Lett*, 2023, **16**, 52.
134. S. Kwon, Y. T. Kwon, Y. S. Kim, H. R. Lim, M. Mahmood and W. H. Yeo, *Biosens. Bioelectron.*, 2020, **151**, 111981.
135. Z. Li, Q. Zheng, Z. L. Wang and Z. Li, *Research (Wash D C)*, 2020, **2020**, 8710686.
136. D. N. Zhao, J. T. Zhuo, Z. T. Chen, J. J. Wu, R. Ma, X. J. Zhang, Y. F. Zhang, X. Wang, X. S. Wei, L. X. Liu, C. F. Pan, J. X. Wang, J. Yang, F. Yi and G. W. Yang, *Nano Energy*, 2021, **90**, 106580.
137. F. Sheng, B. Zhang, Y. Zhang, Y. Li, R. Cheng, C. Wei, C. Ning, K. Dong and Z. L. Wang, *ACS Nano*, 2022, **16**, 10958-10967.
138. Y. Zhang, H. Tu, R. Wu, A. Patil, C. Hou, Z. Lin, Z. Meng, L. Ma, R. Yu, W. Yu and X. Y. Liu, *Biomacromolecules*, 2020, **21**, 4169-4179.
139. S. Zhang, R. J. Tan, K. Zhang, S. Meng, X. Y. Xu, Q. Zhang, C. W. Zhi, Z. Wang, X. S. Liang, S. S. Zhu, Y. L. Tai and J. L. Hu, *Nano Energy*, 2024, **125**, 109548.
140. H. Ouyang, Z. Li, M. Gu, Y. Hu, L. Xu, D. Jiang, S. Cheng, Y. Zou, Y. Deng, B. Shi, W. Hua, Y. Fan, Z. Li and Z. Wang, *Adv. Mater.*, 2021, **33**, e2102302.
141. X. Xiao, Y. Fang, X. Xiao, J. Xu and J. Chen, *ACS Nano*, 2021, **15**, 18633-18646.
142. S. Parandeh, N. Etemadi, M. Kharaziha, G. R. Chen, A. Nashalian, X. Xiao and J. Chen, *Adv. Funct. Mater.*, 2021, **31**, 2105169.
143. J. Sun, A. Yang, C. Zhao, F. Liu and Z. Li, *Sci Bull (Beijing)*, 2019, **64**, 1336-1347.

144. T. Tat, G. Chen, X. Zhao, Y. Zhou, J. Xu and J. Chen, *ACS Nano*, 2022, **16**, 13301-13313.
145. Y. K. Pang, X. C. Xu, S. E. Chen, Y. H. Fang, X. D. Shi, Y. M. Deng, Z. L. Wang and C. Y. Cao, *Nano Energy*, 2022, **96**, 107137.
146. B. B. Chu, X. Qin, Q. Q. Zhu, H. Y. Wang, Z. Wen, X. H. Sun, Y. He and S. T. Lee, *Nano Energy*, 2022, **100**, 107471.
147. C. Wu, P. Jiang, W. Li, H. Guo, J. Wang, J. Chen, M. R. Prausnitz and Z. L. Wang, *Adv. Funct. Mater.*, 2019, **30**, 1907378.
148. T. He, H. Wang, J. Wang, X. Tian, F. Wen, Q. Shi, J. S. Ho and C. Lee, *Adv Sci (Weinh)*, 2019, **6**, 1901437.
149. G. Yao, D. Jiang, J. Li, L. Kang, S. Chen, Y. Long, Y. Wang, P. Huang, Y. Lin, W. Cai and X. Wang, *ACS Nano*, 2019, **13**, 12345-12356.
150. H. Ouyang, Z. Liu, N. Li, B. Shi, Y. Zou, F. Xie, Y. Ma, Z. Li, H. Li, Q. Zheng, X. Qu, Y. Fan, Z. L. Wang, H. Zhang and Z. Li, *Nat Commun*, 2019, **10**, 1821.
151. S. W. Chen, S. M. Huang, H. S. Wu, W. P. Pan, S. M. Wei, C. W. Peng, I. C. Ni, B. T. Murti, M. L. Tsai, C. I. Wu and P. K. Yang, *Adv Sci (Weinh)*, 2022, **9**, e2201507.
152. W. Yan, C. Q. Dong, Y. Z. Xiang, S. Jiang, A. Leber, G. Loke, W. X. Xu, C. Hou, S. F. Zhou, M. Chen, R. Hu, P. P. Shum, L. Wei, X. T. Jia, F. Sorin, X. M. Tao and G. M. Tao, *Mater. Today*, 2020, **35**, 168-194.
153. K. Yao, Q. Zhuang, Q. Zhang, J. Zhou, C. K. Yiu, J. Zhang, D. Ye, Y. Yang, K. W. Wong, L. Chow, T. Huang, Y. Qiu, S. Jia, Z. Li, G. Zhao, H. Zhang, J. Zhu, X. Huang, J. Li, Y. Gao, H. Wang, J. Li, Y. Huang, D. Li, B. Zhang, J. Wang, Z. Chen, G. Guo, Z. Zheng and X. Yu, *Sci Adv*, 2024, **10**, eadq9575.
154. J. Xiong, J. Chen and P. S. Lee, *Adv. Mater.*, 2021, **33**, e2002640.
155. H. Lin and C. Tang, *IEEE Transactions on Intelligent Transportation Systems*, 2022, **23**, 9869-9882.
156. J. H. Syu, M. E. Wu, G. Srivastava, C. F. Chao and J. C. W. Lin, *Ieee Internet of Things Journal*, 2021, **8**, 10347-10355.
157. G. Chen, Y. Li, M. Bick and J. Chen, *Chem Rev*, 2020, **120**, 3668-3720.
158. X. Cao, C. Ye, L. Cao, Y. Shan, J. Ren and S. Ling, *Adv. Mater.*, 2023, **35**, e2300447.
159. S. L. Zhang, M. Bick, X. Xiao, G. R. Chen, A. Nashalian and J. Chen, *Matter*, 2021, **4**, 845-887.
160. X. Peng, K. Dong, C. Ye, Y. Jiang, S. Zhai, R. Cheng, D. Liu, X. Gao, J. Wang and Z. L. Wang, *Sci Adv*, 2020, **6**, eaba9624.
161. H. Yang, J. Li, X. Xiao, J. Wang, Y. Li, K. Li, Z. Li, H. Yang, Q. Wang, J. Yang, J. S. Ho, P. L. Yeh, K. Mouthaan, X. Wang, S. Shah and P. Y. Chen, *Nat Commun*, 2022, **13**, 5311.
162. X. H. Ge, N. Hu, F. J. Yan and Y. Wang, *Nano Energy*, 2023, **112**, 108444.
163. Y. Y. Li, C. H. Wei, Y. Jiang, R. W. Cheng, Y. H. Zhang, C. Ning, K. Dong and Z. L. Wang, *Advanced Fiber Materials*, 2022, **4**, 1584-1594.
164. Y. Li, J. Q. Xiong, J. Lv, J. Chen, D. C. Gao, X. X. Zhang and P. S. Lee, *Nano*

DOI: 10.1039/D5EE00144G

Energy, 2020, **78**, 105358.
165. C. H. Wei, R. W. Cheng, C. Ning, X. Y. Wei, X. Peng, T. M. Lv, F. F. Sheng, K. Dong and Z. L. Wang, *Adv. Funct. Mater.*, 2023, **33**, 2303562.
166. C. Dong, A. Leber, T. Das Gupta, R. Chandran, M. Volpi, Y. Qu, T. Nguyen-Dang, N. Bartolomei, W. Yan and F. Sorin, *Nat Commun*, 2020, **11**, 3537.
167. Y. P. Mao, F. X. Sun, Y. S. Zhu, C. J. Jia, T. M. Zhao, C. R. Huang, C. X. Li, N. Ba, T. T. Che and S. Chen, *Sustainability*, 2022, **14**, 6944.
168. J. Luo, Z. Wang, L. Xu, A. C. Wang, K. Han, T. Jiang, Q. Lai, Y. Bai, W. Tang, F. R. Fan and Z. L. Wang, *Nat Commun*, 2019, **10**, 5147.
169. C. Ning, C. H. Wei, F. F. Sheng, R. W. Cheng, Y. Y. Li, G. Q. Zheng, K. Dong and Z. L. Wang, *Nano Research*, 2023, **16**, 7518-7526.
170. D. Bhatia, S. H. Jo, Y. Ryu, Y. Kim, D. H. Kim and H. S. Park, *Nano Energy*, 2021, **80**, 105508.
171. Z. Lu, C. Jia, X. Yang, Y. Zhu, F. Sun, T. Zhao, S. Zhang and Y. Mao, *Nanomaterials (Basel)*, 2022, **12**, 1576.
172. D. Wu, W. T. Feng, T. Li and Z. Yang, *Data & Knowledge Engineering*, 2023, **148**, 102218.
173. Z. Yu, M. Chen, Y. Wang, J. Zheng, Y. Zhang, H. Zhou and D. Li, *ACS Appl Mater Interfaces*, 2021, **13**, 26981-26988.
174. E. Kovalska, H. T. Lam, Z. Saadi, R. Mastria, A. I. S. Neves, S. Russo and M. F. Craciun, *Nano Energy*, 2024, **128**, 109109.
175. Q. Shi, Z. Zhang, Y. Yang, X. Shan, B. Salam and C. Lee, *ACS Nano*, 2021, **15**, 18312-18326.
176. Q. Shi, Z. Zhang, T. He, Z. Sun, B. Wang, Y. Feng, X. Shan, B. Salam and C. Lee, *Nat Commun*, 2020, **11**, 4609.
177. L. Nicholls, Y. Strengers and J. Sadowski, *Nature Energy*, 2020, **5**, 180-182.
178. W. Gong, X. Wang, W. Yang, J. Zhou, X. Han, M. D. Dickey, Y. Su, C. Hou, Y. Li, Q. Zhang and H. Wang, *Adv. Mater.*, 2021, **33**, e2007352.
179. J. Shi, S. Liu, L. Zhang, B. Yang, L. Shu, Y. Yang, M. Ren, Y. Wang, J. Chen, W. Chen, Y. Chai and X. Tao, *Adv. Mater.*, 2020, **32**, e1901958.
180. R. Wu, S. Seo, L. Ma, J. Bae and T. Kim, *Nanomicro Lett*, 2022, **14**, 139.
181. T. Jin, Z. Sun, L. Li, Q. Zhang, M. Zhu, Z. Zhang, G. Yuan, T. Chen, Y. Tian, X. Hou and C. Lee, *Nat Commun*, 2020, **11**, 5381.
182. F. Wen, Z. Zhang, T. He and C. Lee, *Nat Commun*, 2021, **12**, 5378.
183. Z. X. Zhang, T. Y. Y. He, M. L. Zhu, Z. D. Sun, Q. F. Shi, J. X. Zhu, B. W. Dong, M. R. Yuce and C. K. Lee, *Npj Flexible Electronics*, 2020, **4**, 29.
184. N. Konow, A. Collias and A. A. Biewener, *Front Physiol*, 2020, **11**, 143.
185. J. Suo, Y. Liu, J. Wang, M. Chen, K. Wang, X. Yang, K. Yao, V. A. L. Roy, X. Yu, W. A. Daoud, N. Liu, J. Wang, Z. Wang and W. J. Li, *Adv Sci (Weinh)*, 2024, **11**, e2305025.
186. J. P. Lee, H. Jang, Y. Jang, H. Song, S. Lee, P. S. Lee and J. Kim, *Nat Commun*, 2024, **15**, 530.
187. S. Shen, J. Yi, Z. Sun, Z. Guo, T. He, L. Ma, H. Li, J. Fu, C. Lee and Z. L.

View Article Online
DOI: 10.1039/D5EE00144G

Wang, *Nanomicro Lett*, 2022, **14**, 225.
188. W. Wang, A. F. Yu, J. Y. Zhai and Z. L. Wang, *Advanced Fiber Materials*, 2021, **3**, 394-412.
189. D. Y. Wang, D. Z. Zhang, J. Y. Guo, Y. Q. Hu, Y. Yang, T. H. Sun, H. Zhang and X. H. Liu, *Nano Energy*, 2021, **89**, 106410.
190. S. Sardana, H. Kaur, B. Arora, D. K. Aswal and A. Mahajan, *ACS Sens*, 2022, **7**, 312-321.
191. Y. Chang, S. Xu, B. Dong, J. Wei, X. Le, Y. Ma, G. Zhou and C. Lee, *Nano Energy*, 2021, **89**, 106446.
192. D. Y. Wang, D. Z. Zhang, M. C. Tang, H. Zhang, F. J. Chen, T. Wang, Z. Li and P. P. Zhao, *Chem. Eng. J.*, 2022, **446**, 136914.
193. M. C. Turner, Z. J. Andersen, A. Baccarelli, W. R. Diver, S. M. Gapstur, C. A. Pope, 3rd, D. Prada, J. Samet, G. Thurston and A. Cohen, *CA Cancer J Clin*, 2020, **70**, 460-479.
194. M. Cho, V. Hiremath and J. G. Seo, *Atmospheric Environment: X*, 2021, **12**, 100138.
195. J. Liu, T. Jiang, X. Li and Z. L. Wang, *Nanotechnology*, 2019, **30**, 292001.
196. A. Vázquez-López, X. Ao, J. Sánchez del Río Saez and D.-Y. Wang, *Nano Energy*, 2023, **114**, 108635.
197. M. Kang, N. Y. Jang, Y. J. Kim, H. J. Ro, D. Kim, Y. Kim, H. T. Kim, H. M. Kwon, J. H. Ahn, B. O. Choi, N. H. Cho and S. W. Kim, *Cell Rep Phys Sci*, 2022, **3**, 100813.
198. L. Wang, Y. Bian, C. K. Lim, Z. Niu, P. K. H. Lee, C. Chen, L. Zhang, W. A. Daoud and Y. Zi, *Nano Energy*, 2021, **85**, 106015.
199. Z. Peng, J. Shi, X. Xiao, Y. Hong, X. Li, W. Zhang, Y. Cheng, Z. Wang, W. J. Li, J. Chen, M. K. H. Leung and Z. Yang, *Nat Commun*, 2022, **13**, 7835.
200. Y. Cho, Y. Son, J. Ahn, H. Lim, S. Ahn, J. Lee, P. K. Bae and I. D. Kim, *ACS Nano*, 2022, **16**, 19451-19463.
201. C. Wang, Y. C. Chen, H. T. Hsu, Y. F. Tsao, Y. C. Lin, C. F. Dee and E. Y. Chang, *Materials (Basel)*, 2021, **14**, 6558.
202. B. Yuan, J. Wan, Y.-H. Wu, D.-Q. Zou and H. Jin, *Journal of Computer Science and Technology*, 2023, **38**, 228-247.
203. J. Silva, N. Rosa and F. Aires, *Journal of Universal Computer Science*, 2024, **30**, 502-530.
204. C. K. Qiu, F. Wu, C. Lee and M. R. Yuce, *Nano Energy*, 2020, **70**, 104456.
205. K. Lee and K. Yim, *Sensors (Basel)*, 2023, **23**, 3501.
206. P. Maharjan, K. Shrestha, T. Bhatta, H. Cho, C. Park, M. Salauddin, M. T. Rahman, S. S. Rana, S. Lee and J. Y. Park, *Adv Sci (Weinh)*, 2021, **8**, e2100711.
207. J. Yi, K. Dong, S. Shen, Y. Jiang, X. Peng, C. Ye and Z. L. Wang, *Nanomicro Lett*, 2021, **13**, 103.
208. F. J. Xing, Z. Q. Ou, X. B. Gao, B. D. Chen and Z. L. Wang, *Adv. Funct. Mater.*, 2022, **32**, 2205275.
209. R. Cheng, K. Dong, L. Liu, C. Ning, P. Chen, X. Peng, D. Liu and Z. L. Wang,

View Article Online
DOI: 10.1039/D5EE00144G

ACS Nano, 2020, **14**, 15853-15863.

210. L. Y. Ma, R. H. Wu, A. Patil, J. Yi, D. Liu, X. W. Fan, F. F. Sheng, Y. F. Zhang, S. Liu, S. Shen, J. Wang and Z. L. Wang, *Adv. Funct. Mater.*, 2021, **31**, 2102963.
211. T. Chen, W. Z. Song, M. Zhang, D. J. Sun, D. S. Zhang, C. L. Li, W. Y. Cui, T. T. Fan, S. Ramakrishna and Y. Z. Long, *RSC Adv*, 2023, **13**, 11697-11705.
212. H. He, J. Liu, Y. Wang, Y. Zhao, Y. Qin, Z. Zhu, Z. Yu and J. Wang, *ACS Nano*, 2022, **16**, 2953-2967.
213. L. Ma, R. Wu, S. Liu, A. Patil, H. Gong, J. Yi, F. Sheng, Y. Zhang, J. Wang, J. Wang, W. Guo and Z. L. Wang, *Adv. Mater.*, 2020, **32**, e2003897.
214. S. Divya, S. Panda, S. Hajra, R. Jeyaraj, A. Paul, S. H. Park, H. J. Kim and T. H. Oh, *Nano Energy*, 2023, **106**, 108084.

View Article Online
DOI: 10.1039/D5EE00144G

Data availability

No primary research results, software or code, have been included and no new data was generated or analyzed as part of this review.